Article Type: Article

Running head: Controls on otolith chemistry

Title: Coupling biogeochemical tracers with fish growth reveals physiological and environmental controls on otolith chemistry

Gretchen L. Grammer[1*], John R. Morrongiello[2], Christopher Izzo[1,3], Peter J. Hawthorne[4], John F. Middleton[4], and Bronwyn M. Gillanders[1]

[1]Southern Seas Ecology Laboratories, School of Biological Sciences, The University of Adelaide, SA 5005, Australia

[2]School of BioSciences, The University of Melbourne, VIC 3010, Australia

[3]Fisheries Research and Development Corporation, Adelaide, SA 5000, Australia

[4]South Australian Research and Development Institute (Aquatic Sciences), West Beach, SA 5024, Australia

* Corresponding Author. Email: gretchen.grammer@sa.gov.au. Current affiliation: South Australian Research and Development Institute (Aquatic Sciences), 2 Hamra Ave., West Beach, SA 5024, Australia

Abstract:

Biogeochemical tracers found in the hard parts of organisms are frequently used to answer key ecological questions by linking the organism with the environment. However, the biogeochemical relationship between the environment and the biogenic structure becomes less predictable in higher organisms as physiological processes become more complex. Here, we use the simultaneous combination of biogeochemical tracers and fish growth analyzed

with a novel modeling framework to describe physiological and environmental controls on otolith chemistry in an upwelling zone. First, we develop increasingly complex univariate mixed models to describe and partition intrinsic (age effects) and extrinsic (environmental parameters) factors influencing fish growth and otolith element concentrations through time. Second, we use a multivariate mixed model to investigate the directionality and strength between element-to-element and growth relationships and test hypotheses regarding physiological and environmental controls on element assimilation in otoliths. We apply these models to continuous element (Na, Sr, Mg, Ba, Li) and growth increment profiles (monthly resolution over 17 years) derived from otoliths of reef ocean perch (*Helicolenus percoides*), a wild-caught, site-attached, fully marine fish. With a conceptual model, we hypothesize that otolith traits (elements and growth) driven by environmental conditions will correlate both within an otolith, reflecting the time dependency of growth and element assimilation, and among individuals that experience a similar set of external conditions. We found some elements (Sr:Ca and Na:Ca) are mainly controlled by physiological processes, while other elements (Ba:Ca and Li:Ca) are more environmentally influenced. Within an individual fish, the strength and direction of correlation varies among otolith traits, particularly those under environmental control. Correlations among physiologically regulated elements tend to be stronger than those primarily controlled by environmental drivers. Surprisingly, only Ba:Ca and growth are significantly correlated among individuals. Failure to appropriately account for intrinsic effects (e.g. age) led to inflated estimates of among individual correlations and a depression of within individual correlations. Together, the lack of among-individual correlations of otolith traits in properly formulated models and the biases that can be introduced by not including appropriate intrinsic covariates suggest that caution is needed when assuming multi-elemental signatures are reflective solely of shared environments.

Key words: bioarchive, biogeochemical, growth, microchemistry, fish, otolith, physiology, sclerochronology, sclerochemistry, mixed effects modeling, upwelling, *Helicolenus*

Introduction:

How does environmental variation influence a species' biology? Can we use this insight to hindcast past conditions and forecast future states? These are key ecological questions asked

by many researchers, but to answer them we need to address two fundamental points: 1) data must be collected at the appropriate resolution and spatio-temporal scale; and 2) measurements need to actually inform the question at hand. Biogeochemical tracers (e.g. trace elements, stable isotopes, chemical pollutants, lipids) are commonly used to make the link between an organism and the environment. There remain, however, a number of outstanding issues around their use in ecological studies because each tracer has a unique set of properties, controls and assumptions (Rubenstein and Hobson 2004, Ramos and González-Solís 2012). Furthermore, different tracers reflect different biological/ecological processes. Thus, it is desirable to simultaneously measure multiple biogeochemical tracers as well as the effects of growth or other physiological factors to allow for synergistic interactions to be explored and understood (Ethier et al. 2010, Ramos and González-Solís 2012, Cresson et al. 2015).

Elements are frequently used as biogeochemical tracers in biogenic structures to make inferences about past environments (e.g. Montaggioni et al. 2006, Batenburg et al. 2011) or organismal movement across environmental gradients (e.g. Parrish et al. 1983, Elsdon and Gillanders 2003a, Ethier et al. 2014). Key assumptions underpinning these corollaries rely on the predictability of element assimilation relative to the surrounding environment and minimal or constant influence of biological effects ('vital effects'). However, the biogeochemical relationship between the environment and the biogenic structure becomes less predictable in higher organisms as physiological processes become more complex (Weiner and Dove 2003, Stanley 2006, Cusack and Freer 2008).

Understanding and accounting for physiological processes allow biological and environmental influences on element assimilation to be disentangled and the tracer to become ecologically useful. Early research on otoliths (fish earstones) from the 1980s and 1990s focused on differentiating the effects of biological and environmental controls upon element composition (Kalish 1989, 1991, Campana 1999). Recently, there has been renewed interest in this area (e.g. Sturrock et al. 2014, Sturrock et al. 2015), as complex and conflicting results have been revealed between otolith chemistry and ambient water (Thresher 1999, Elsdon et al. 2008, Brown and Severin 2009). These issues need to be resolved if we are to have confidence in the use of otolith chemistry as an environmental proxy.

Fish otoliths are biogenic structures readily accessible in almost every aquatic environment. These structures contain growth increments that can be time resolved, making them one of the most extensively studied calcified structures of a higher organism. Distinct biogeochemical (here-after referred to as chemistry or chemical) profiles found in otoliths are assumed to reflect the fish's ambient environment (e.g. Elsdon and Gillanders 2002, 2003b, de Vries et al. 2005). Otolith chemical profiles are widely used as natural tags to examine stock structure, population connectivity, and movement patterns through different aquatic environments (e.g. Gillanders 2002, Elsdon and Gillanders 2003a, Reis-Santos et al. 2013). They are also used as paleoproxies to infer past environments (Disspain et al. 2011, Disspain et al. 2015, Izzo et al. 2016).

Otoliths are encapsulated in the fish's head, surrounded by endolymph, and are not in direct contact with the environment (Campana 1999). This places a first order limit on the responsiveness of otolith chemistry to variations in ambient water chemistry (Sturrock et al. 2014). Fluctuations in the physical environment (e.g. temperature, salinity, current strength) directly affect fish physiology by altering metabolism, respiratory function, osmotic processes, feeding behavior and/or diet (Brett and Groves 1979, Brown et al. 2004, Wootton 2011). Likewise, reproduction and growth affect fish physiology, and together these processes can cause otolith chemistry to respond both directly or indirectly to changes in the ambient environment (Walther et al. 2010, Sturrock et al. 2014, Sturrock et al. 2015). Furthermore, the amount of physiological regulation varies between elements and environments. For example, Ba, Mg, and Li in blood plasma of marine fish display the least amount of biological fractionation compared to Sr (Sturrock et al. 2014), and concentrations of Sr:Ca (Sr normalized to Ca) in otoliths are linked to reproductive processes (Kalish 1991, Sturrock et al. 2015). A meta-analysis on Sr:Ca assimilation into otoliths revealed that Sr:Ca incorporation in marine species is more likely to be physiological in nature, but physiological factors have little to no effect on Sr:Ca incorporation in freshwater or diadromous fish species (Brown and Severin 2009).

Most research examining physiological controls on otoliths is laboratory based and primarily targets early life history stages for limited experimental durations (i.e. days to weeks; but see Kalish 1991, Sturrock et al. 2014, Sturrock et al. 2015). These experiments likely do not capture physiological processes unique to adults, such as reproduction. Moreover, laboratory based results may not accurately represent the same responses in wild caught fish (Elsdon and

Gillanders 2005). Extensive field-based studies that naturally integrate environmental and physiological processes are therefore required to understand the controls of tracers.

Here, we develop a conceptual model around element concentrations and growth correlations within a fish's otolith and among different fish inhabiting the same marine environment (Figure 1). We consider the minor elements of Na, Sr and trace elements of Mg, Ba, and Li (all normalized to Ca). We propose, underpinned by current understanding, that certain elements assimilated into otoliths are primarily under physiological control, environmental control or both. We hypothesize that Na:Ca and Sr:Ca will be predominantly influenced by an individual's physiology, while Ba:Ca and Li:Ca would be primarily affected by environmental parameters (Figure 1). We also predict growth rate and Mg:Ca would be moderately influenced by both physiology and the environment. It is likely that there will be stronger correlations within physiological or environmental variables (elements or growth), but less so between the two groups due to the different controls on element assimilation or growth. Furthermore, the level at which correlation occurs (within or among individuals) will vary among physiologically and environmentally controlled variables. Those elements most influenced by physiological processes, such as reproduction or metabolic processes, are expected to be correlated within an otolith as they reflect processes intrinsic to the individual ('vital effects'). Conversely, variables driven by environmental conditions will correlate both within an otolith, reflecting the time dependency of growth and element assimilation, and among individual fish that experience a similar set of external conditions (Figure 1).

We test these hypotheses using the reef ocean perch (*Helicolenus percoides* (Richardson, 1842); here after referred to as 'ocean perch'), a long-lived, benthic fish found in continental marine waters of southern Australia and New Zealand. We focused on this species for both biological (i.e. longevity, non-migratory, benthic, fully marine) and environmental reasons. Ocean perch for this study were collected from a region dominated by seasonal upwelling (Figure 2a). Upwelling is a wind-driven, oceanographic process that brings cold, nutrient-rich, deep-water masses to the ocean's surface (Botsford et al. 2003). Upwelled waters typically leave distinctive elemental signatures in biological carbonates due to differences in water mass chemistry and associated links to primary productivity (e.g. coral: Lea et al. 1989, otoliths: Kingsford et al. 2009, mollusks: Hatch et al. 2013). For example, where sources of upwelled water are enriched with Ba from deep water (e.g. Galapagos Island, outer Great Barrier Reef, central California coast), coral skeletons (Lea et al. 1989, Walther et al. 2013)

and otoliths (Kingsford et al. 2009, Woodson et al. 2013) show spikes in concentrations of Ba:Ca during upwelling periods. Coastal upwelling events along Australia's southern coast are distinct, seasonal occurrences (austral summer: December to March; Middleton and Bye 2007) that provide much needed nutrients to the oligotrophic waters of this region (Nieblas et al. 2009, van Ruth et al. 2010).

We first develop a series of increasingly complex, univariate mixed-effects models to partition variation in otolith elemental concentration or growth between intrinsic (e.g. individual, age) and extrinsic (e.g. local upwelling, temperature) drivers (Weisberg et al. 2010, Morrongiello and Thresher 2015). We apply these models to continuous, multi-year, otolith chemistry and otolith growth increment profiles derived from our test species, a wild-caught, site-attached, fully marine fish. We then develop a novel multivariate mixed-effect model, based on the univariate models, to generate estimates of between element/growth correlations within and among individuals and investigate the strength and directionality of those relationships. These estimates are conditional on intrinsic effects. We use the strong, local upwelling signal as an extrinsic cue to explore synergistic effects of age and environment on chemical assimilation into the otolith and on fish growth.

Methods:

Oceanographic setting & study species

In the southeastern Indian Ocean, upwelling occurs along the Bonney Coast of southern Australia in the austral summer as two to four upwelling events, each lasting three to ten days in duration, interspersed by episodes of weak downwelling and surface water mixing (Kämpf et al. 2004, Middleton and Bye 2007). These upwelling areas are wind-forced and influenced by the Flinders Current flowing westward along the shelf-slope of southern Australia (Middleton and Bye 2007). The Flinders Current results from wind curl stress and the equatorward Sverdrup transport of water in the Southern Ocean; it is similar to larger western boundary currents but is part of a northern boundary current system that produces upwelling areas (Middleton and Cirano 2002, Middleton and Bye 2007). A reversal in current strength occurs in the winter months of southern Australia where an eastward flowing current, the Leeuwin Current, becomes dominant and produces downwelling. Both the Flinders and Leeuwin Current systems are wind-dominated, which causes the seasonal strengthening or weakening of either current system (Middleton and Bye 2007, James and Bone 2011).

Ocean perch were collected from the upwelling area along the Bonney Coast of southern Australia (near 37°40'S, 139°50'E; Figure 2a) at depths between 43 and 119 m (mean: 80 m). Ocean perch are lecithotrophic (live bearing; Pavlov and Emel'yanova 2013) and demersal as both juveniles and adults (Park 1993, Smith et al. 2009). Juveniles and adults are benthopelagic omnivores (Bulman et al. 2001) with ontogenetic diet shifts from smaller crustaceans (mysids and galatheids) to larger crustaceans (scampi and two-spine crab; Horn et al. 2012). Benthic fish and salps (carcasses as food-fall; Henschke et al. 2013) are also important dietary components for all ages (Bulman et al. 2001, Horn et al. 2012).

Otolith preparation

Ocean perch were caught from October 2011 to January 2013 and ranged in size from 160 to 344 mm total length (TL). Sagittal otoliths were removed from the fish, cleaned in ultrapure water and stored dry. One otolith from each fish was embedded in epoxy resin, transversely thin sectioned to include the primordium, polished with lapping film, and mounted on a microscope slide using thermoplastic cement (Figure 2b). Both the epoxy resin and thermoplastic cement were spiked with indium chloride as an indicator of those substances. Slides were cleaned in ultrapure water and air dried.

Analysis of elemental otolith chemistry

Concentrations of elements were measured in the otolith from the core to the proximal, dorsal edge (Figure 2b) using a Resonetics M-50-LR 193nm Excimer laser ablation system coupled to an Agilent 7700cx quadrupole ICP-MS (housed at Adelaide Microscopy, The University of Adelaide). The laser was operated at a scan speed of 4 $\mu m \cdot s^{-1}$ with a frequency of 10 Hz using a 33 µm diameter to produce continuous laser transects across the otoliths. Prior to each ablation, background levels of elements in the ablation chamber were measured for 30 s and a pre-ablation path 45 µm diameter was made. Instrument drift and precision was measured by analyzing a reference standard (NIST 612) after about every 10 samples and a carbonate standard (MACS 3; US Geological Survey) at the beginning and end of each laser session (≈5 hrs). Dual transects were ablated on each otolith to allow the laser to be optimized for higher and lower concentration elements (Figure 2b). Higher concentration elements measured were ^{23}Na (dwell time: 50 ms), ^{88}Sr (100 ms), ^{24}Mg (100 ms) and ^{138}Ba (100 ms). ^{7}Li (150 ms) was the only lower concentration element measured. For both transects, ^{43}Ca (5 ms), ^{44}Ca (5 ms) and ^{115}In (high concentration: 10 ms; low concentration: 5 ms) were also measured to

produce element:Ca ratios and confirm otolith material was constantly ablated. Precision, calculated as the mean coefficients of variation (CV) of repeated measures, for all elements based on the NIST 612 standard was <1%. Precision for the higher concentration elements based on the MACS 3 standard was <3.1% and <1% for the lower concentration element, Li. Raw data were processed using GLITTER software (Griffin et al. 2008) and all elements were normalized to Ca and presented as element:Ca (mmol/mol).

Monthly resolution of growth increments and element:Ca profiles

Ablated otolith sections (n = 38) were viewed with a compound microscope and digital camera system (×87.5 magnification; Leica DFC320 digital camera) for age interpretation and growth increment measurement. Along each ablation path, the annual growth increments were marked and measured (in mm; Image-Pro Plus v. 7.0, Media Cybernetics); then, the hyaline and opaque zones were measured within each annual increment. The proportion of hyaline to opaque material within an annual growth increment was about 50%. We designated the hyaline growth zone as forming from November to March (5 months) and the opaque zones as being deposited from April to October (7 months). These timeframes are based on ocean perch age data from age validations (Paul and Horn 2009), marginal increment analysis (Park 1993), and the status of the otolith's marginal edge at the time of capture in the current study. Ages of ocean perch have been validated and each annual growth increment is comprised of one opaque growth zone and one hyaline growth zone (Paul and Horn 2009). Ocean perch from the Bonney Upwelling region were assigned a birthdate of October 1 based on the peak spawning season (September to November) of ocean perch in southeastern Australia (Park 1993).

We assigned each annual growth increment a year relative to the date of capture taking into account the marginal increment. Then, starting at the outer edge of the opaque core region (represents transition of growth at end of fish's first winter; Paul and Horn 2009) and progressing towards the otolith's edge, the hyaline and opaque zones were resolved to monthly increments by dividing the total measurement of each zone by its corresponding number of months, e.g. hyaline measurement divided by five months or opaque measurement divided by seven months. The element:Ca transect data were resolved in a similar fashion. Since the laser was operated in a time resolved mode, we used the scan speed ($\mu m \cdot s^{-1}$) to convert each time dated element:Ca data point (s) to a distance measurement (µm). Next, we aligned these data to the growth increment measurements using the otolith edge as the

reference point to assign appropriate years. Finally, we resolved the element:Ca data to monthly increments as above, starting at the outer edge of the opaque core region and progressing outwards. The element:Ca transect data and growth measurements were trimmed to only include years 2 to 7 (maximum). This allowed certainty of the starting point of the data when resolving to monthly increments (year 2 begins at the edge of opaque core region) and provided at least two element:Ca data points for each month. Generally after year 7, the width of the monthly growth increment decreased to the point where the laser scan speed, coupled with the ablation diameter, was equal to or greater than that increment width. Because growth was resolved to monthly increments on both the low concentration and high concentration elemental transects, these measurements were averaged and combined into one growth transect (*Growth*) for subsequent analyses. Data collected from at least five fish made up each monthly time increment for all element:Ca and growth increment profiles (number of fish contributing to a time increment: mean: 11, max: 17).

Univariate mixed modeling to estimate intrinsic and extrinsic variation

We developed six univariate mixed models for the monthly resolved element:Ca (*Na:Ca, Sr:Ca, Mg:Ca, Ba:Ca, Li:Ca*) and growth (*Growth*) data extracted from the otoliths to examine relationships with upwelling events. These models enabled us to partition monthly variation of the response variables (*Na:Ca, Sr:Ca, Mg:Ca, Ba:Ca, Li:Ca* or *Growth*) between intrinsic (e.g. age) and extrinsic (e.g. upwelling index) drivers (Weisberg et al. 2010, Morrongiello et al. 2014). The intrinsic covariates were fish age in months (*Age*) and age in months at capture (*age.month.cap*), whilst extrinsic variables describe monthly characteristics of upwelling: an upwelling index (*Bonney UI*), bottom temperature (*Bottom Temp*) and levels of chlorophyll a (*Chl-a*) (full descriptions in Table 1). As expected from upwelling physics, the *Bonney UI* correlated negatively with *Bottom Temp* (r: -0.410, p<0.001) and positively with *Chl-a* (r: 0.340, p<0.001); *Chl-a* was negatively correlated with *Bottom Temp* (r: -0.320, p<0.001).

Following the two-stage procedure of Morrongiello and Thresher (2015), we first developed a series of linear mixed-effect models that combined fixed intrinsic variables (*Age*, *age.month.cap*) with different random effect structures in a hierarchical manner to isolate sources of variation in otolith element concentrations or fish growth (Table 2). Second, we introduced extrinsic environmental variables into the resulting best models to relate the observed variability to the environment. We used R 3.0.3 with the packages of 'lme4' ('lmer'

297 function; Bates et al. 2014), 'effects' (Fox et al. 2014), and 'AICcmodavg' (Mazerolle 2015)
298 to perform model analyses (R Development Core Team 2014), and the 'Hmisc' package
299 ('rcorr' function; Harrell 2014) to compare among upwelling variables with pairwise
300 Pearson's correlation coefficients. All response variables and *Age* were natural-log
301 transformed to meet model assumptions of normality and homogeneity of variance, and fixed
302 predictor variables were mean centered to assist model convergence (Morrongiello et al.
303 2014, Morrongiello and Thresher 2015). Akaike's Information Criterion (*AIC*) corrected for
304 small sample sizes (*AICc*) was used to test relative support for each model (Burnham and
305 Anderson 2004). We also used marginal and conditional R^2 metrics for mixed effects models
306 (Nakagawa and Schielzeth 2013, Johnson 2014) to estimate the proportion of variance for
307 fixed effects alone and combined fixed and random effects, respectively.
308
309 The element:Ca and growth data were comprised of repeated monthly measures (element
310 concentrations or growth increment width) from each individual across multiple years.
311 Random effects structures (n = 4; Table 2) contained random intercepts for *FishID* and *Month*
312 (see Table 1 for descriptions) in combination with random slopes for *Age*. Random intercepts
313 for *FishID* and *Month* induce correlation among measurements within an individual and
314 correlation among element concentrations or growth increments assimilated in the same
315 month per year, respectively. Individual element concentration or growth was allowed to vary
316 in comparison to the model average by using a *FishID* random intercept. Likewise, a random
317 *Month* intercept gives temporally resolved (month per year) estimates of whether extrinsic
318 drivers provided good or poor conditions for element assimilation or growth relative to the
319 long term mean (Morrongiello et al. 2014, Morrongiello and Thresher 2015). Random slopes
320 for *Age* enabled the fixed effect *Age* - *element:Ca* or *Growth* relationship to vary among
321 individuals and among months per year. Random *Age* slopes for each fish permit a distinct
322 age-dependent element assimilation or growth trajectory while still inferring an age response
323 for the population. Similarly, a random *Age* slope for *Month* allows for age-dependent
324 responses to environmental effects through time (Morrongiello et al. 2014, Morrongiello and
325 Thresher 2015).
326
327 The best random effect structures for the six response variables were selected by adding all
328 fixed intrinsic effects (*Age*, *age.month.cap*) to each possible random effects structure and
329 fitting the models using restricted maximum likelihood estimates of error (REML). The most
330 complex intrinsic effect model took the form:

$$y_{ijkl} = \alpha_0 + \alpha_i^F + \alpha_k^M + \beta_1 x_{ij} + b_{1i}^F x_{ij} + b_{1k}^M x_{jk} + \beta_2 x_l + \varepsilon_{ijk} \quad \text{Eqn. 1}$$

$$\begin{bmatrix} \alpha_i^F \\ b_{1i}^F \end{bmatrix} \sim N(0, \Sigma_i), \qquad \begin{bmatrix} \alpha_k^M \\ b_{1k}^M \end{bmatrix} \sim N(0, \Sigma_k), \qquad \varepsilon_{ijk} \sim N(0, \sigma^2)$$

where y_{ijkl} is a response variable measurement for fish *i* at age *j* from month *k*, caught at age (*age.month.cap*) *l*. α_0 is the overall mean monthly response intercept, α_i^F is the random intrinsic effect for fish *i*, and α_k^Y is the random extrinsic environmental effect for month *k*. β_1 is the fixed effect *Age* coefficient, β_2 is the fixed effect *age.month.cap* coefficient, and b_{1i}^F and b_{1k}^M are random *Age* slopes for fish *i* and month *k* respectively.

Next, the fixed effect structures of either *Age* or *Age* + *age.month.cap* were fit to the best random effects structure (from above) for each response variable with maximum likelihood estimates of error (ML). Each candidate set of models were compared with ΔAICc values. Then, unbiased parameter estimates were produced for each response variable by refitting the best ranked models with REML (Zuur et al. 2009). We estimated the temporal synchrony of element assimilation or growth across individuals by calculating the intraclass correlation coefficient (ICC). The ICC model contained random intercepts for both *FishID* and *Month*, but a random *Age* slope was only included for *FishID* to ensure interpretability of the *Month* variance component (Morrongiello and Thresher 2015). Finally, we added the upwelling specific, environmental covariates (*Bonney UI*, *Bottom Temp*, *Chl-a*; Table 1) to each optimal model to assess extrinsic effects within and among the response variables. We also tested for *Age* specific responses of elements or growth for each environmental covariate by fitting interaction terms.

Multivariate mixed modeling to estimate within and among individual correlations

Because the six response variables represent repeated measures of multiple elements and growth within the same otolith of each fish, it is of interest to estimate correlations among these otolith 'traits' both within and among individuals (response variables here after are referred to as traits). These relationships could be directional (i.e. changes in element x causes proportional changes in element y) or reflective of a common response to a physiological or environmental driver. Within and among otolith trait correlations therefore allows us to estimate the strength of relationships between the elements themselves, as well

as growth, and begin linking these to either physiology (intrinsic effects), the environment (extrinsic effects) or both. It is important to note that the six traits (elements: n = 5; growth: n = 1) are dependent on the same intrinsic and extrinsic drivers at a given time and are not independent of one another. Whilst among-individual correlations can be based on average trait values for each individual derived from the series of univariate models outlined above, these values will be biased due to unaccounted-for within-individual variation and do not properly account for uncertainty around element:Ca or growth estimates (Hadfield et al. 2010, Dingemanse and Dochtermann 2013). Furthermore, such an approach precludes estimating trait correlation within otoliths (e.g. is an increase or decrease in a particular element related to a period of high or low growth during a fish's lifetime). Multivariate mixed-effects models avoid these limitations and allow for the concordant estimation of both within- and among-individual trait variation across multiple traits (Dingemanse and Dochtermann 2013).

We used a multivariate mixed effects linear model fitted in the 'MCMCglmm' package of R (Hadfield 2010) which applies a Bayesian approach to estimate variance-covariance matrices within individuals (**I**) and among individuals (**R**) for all six traits (bold font denotes matrices). These matrices were then used to generate point estimates and 95% credible intervals for each pair-wise within- and among-individual otolith trait correlation; credible intervals that do not overlap zero indicate statistical 'significance'. Multivariate mixed models fit with MCMCglmm can cope with missing response values, which was beneficial as not all otolith traits were measured at each point along an otolith transect (e.g. Li could not be monthly resolved past age 7 due to decreasing otolith growth increment widths and limitations of the laser ablation ICP-MS system).

Similar to univariate analyses, traits were natural log-transformed where necessary to meet assumptions of multivariate normality. They were then standardized (observation-mean/SD) to ensure similar scales, which aids model convergence and parameter interpretation. Our first multivariate mixed model generated conditional correlation estimates (conditioned on intrinsic effects) and included fixed effects for trait-specific *Age* (natural log-transformed) and trait-specific *age.month.cap* terms to account for intrinsic effects on growth and element assimilation into the otolith (Table 1). In all univariate models, a random effect structure allowing for individual- and month-specific differences in the *Age* coefficient performed best (Table 2). We therefore used this random effect structure here as well, adding the additional

complexity that these individual and month random slopes could vary across elements (e.g. an individual might have a steeper than average Na:Ca-age relationship but a shallower than average growth-age relationship). We then developed a second multivariate mixed model to explore the implications of ignoring intrinsic effects (i.e. *Age* and *age.month.cap* terms excluded) when estimating within and among individual correlations amongst otolith traits.

We used parameter expanded priors (Hadfield 2010), ran our model for 110,000 iterations with a burn-in phase of 10,000 and a thinning interval of 25. This resulted in a well-mixed chain, no autocorrelation and a sample size of 4,000 values for each estimate. The assumption of multivariate normality was satisfied with visual inspection of the model's marginal residuals (A). We provide R code and data sets for the univariate and multivariate models in the Supplement.

Results:

Sources of element:Ca and growth variation

The most strongly supported random effects structure for all otolith traits included a random *Age* slope on both *FishID* and *Month* (Table 2), which means the *element:Ca - age* and *Growth - age* relationships vary among individual fish and months. For Sr:Ca, Ba:Ca and Li:Ca, the best fixed effects structure included both *Age* and *age.month.cap* terms, while Na:Ca, Mg:Ca and growth included *Age* only (Table 3). Growth, Ba:Ca, Na:Ca, Mg:Ca and Li:Ca all decreased with age, while Sr:Ca increased with age (Table 3, Figure 3). Older fish at capture had higher overall levels of Ba:Ca and Sr:Ca than younger fish (positive *age.month.cap* slope), while the negative *age.month.cap* slope seen in Li:Ca indicated that younger fish had overall higher Li:Ca levels than older fish (Table 3). These differences suggest older fish most likely have experienced slightly different environmental/dietary conditions during the earlier years of their lives than the younger fish have experienced during that same portion of their own lives. Power functions fit to *element:Ca - age* and *Growth - age* relationships (to facilitate comparison with other studies) estimated assimilation/growth rates (AR: $\mu mol \cdot mol^{-1} \cdot month^{-1}$; GR: μm/month) for ocean perch (Figure 3).

Random variability around mean *element:Ca* or *Growth* was greatest among fish (*FishID*) followed by among months (*Month*) (Table 3). *Element:Ca* or *Growth - Age* slopes had the highest variation among individuals followed by variation among months. All *element:Ca*

data displayed negative correlations between the *Month* random intercept and *Age* slope, signifying that younger fish assimilate higher concentrations of elements compared to older fish when conditions are favorable for element assimilation (older fish assimilate relatively higher concentrations than younger fish when conditions are less favorable for element assimilation; Table 3). A positive correlation between the *Month* random intercept and *Growth* - *Age* slope (slopes are shallower at higher intercepts) indicates older fish are growing proportionally better than younger fish during months of good growth (younger fish grow better in poor times). Random *Age* slopes of the otolith traits were positively correlated with *FishID*, meaning there is variation in growth or element assimilation across individuals (larger *FishID* effects lead to greater growth variation across individuals). Element assimilation of Na:Ca and Sr:Ca varied the least across individuals as they aged (corr: 0.470 and 0.330, respectively), whereas Ba:Ca and Li:Ca varied the most (corr: 0.220 and 0.200, respectively). When compared to element assimilation, growth varied moderately across individuals (corr: 0.310).

Patterns of temporal variation in all otolith traits (extracted from the *Month* random effect term) were cyclical (Figure 4). Na:Ca and Sr:Ca varied the least through time, but displayed clear periodicity. The amount of synchrony seen in each element among individuals in each month ranged from a low ICC of 1.74% (Mg:Ca) to a high of 5.08% (Na:Ca) (Table 3). Growth had the highest ICC of 8.50%, although these estimates are conservative as the best intrinsic effects models included random age slopes for *FishID* and *Month*.

Relating temporal variation of element:Ca and growth data to environmental parameters

Upwelling-specific environmental covariates improved all intrinsic effect models (Table 4). The upwelling index with an age interaction (*Age * Bonney UI*) best explained variation for Na:Ca, Sr:Ca and growth (Table 4). The upwelling index alone (*Bonney UI*) best explained variation for Ba:Ca and Mg:Ca, and chlorophyll-a (*Chl-a*) concentrations significantly improved model fit for Li:Ca (Table 4). Na:Ca, Mg:Ca, and Ba:Ca concentrations were all significantly and negatively related to the upwelling index; in contrast, Sr:Ca and growth were significantly and positively related to the upwelling index (Table 4, Figures 5a-c, g, i). Li:Ca was positively related to monthly chlorophyll-a concentrations (Figure 5h).

The elemental concentrations of younger fish showed a steeper rate of change over the range of environmental variables experienced by fish, suggesting younger fish increase or decrease

element assimilation more rapidly than older fish (Figure 5d-f, j, k). This pattern was reversed when comparing growth at a given age with the upwelling index. Very young fish grew consistently fast across all upwelling conditions, while older fish proportionally increased their growth rate when upwelling increased (Figure 5l).

Estimating within and among individual correlations with multivariate mixed models

Within individual correlations of otolith traits revealed the strength and direction of relationships between the otolith traits (Figure 6a; Appendix S1: Table S1). Growth was weakly correlated with Na:Ca (0.130), Sr:Ca (-0.137), and Mg:Ca (0.128) (Figure 6a; Appendix S1: Table S1), whereas no significant correlation existed between growth and Ba:Ca or Li:Ca within an individual. A moderate, negative correlation was found between Na:Ca and Sr:Ca (-0.396). Mg:Ca was moderately correlated with Ba:Ca (0.313) and weakly correlated with Na:Ca (0.267). Very weak correlations existed between other pairs of traits (Figure 6a; Appendix S1: Table S1).

When comparing otolith traits among individuals, only Ba:Ca and growth were significantly correlated (-0.410; Figure 6a; Appendix S1: Table S2). This suggests that individuals with overall higher growth generally have lower Ba:Ca, but this relationship was not found between monthly increments measured within an individual otolith. All other otolith traits were not correlated among individuals (Figure 6a; Appendix S1: Table S2).

Within individual correlations from the model excluding *Age* and *age.month.cap* were qualitatively similar to those from the more complex model (Figure 6b, Appendix S1: Table S3). The biggest differences were evident among individuals where all 15 correlations were strongly significant (>±0.8, Figure 6c, Appendix S1: Table S4).

Discussion:

Otolith chemistry and fish growth displayed clear cyclic seasonal signals over a 17 year period in a marine system. Age-dependent relationships existed in the element:Ca and growth profiles, and responses to the environment differed as the fish aged. Temporal signals were correlated with seasonal upwelling events. Since elemental concentrations and growth were measured simultaneously within the otolith, direct comparisons among otolith traits, both within and among individual fish, were made through time. Multivariate mixed modeling revealed the strength and direction of relationships between element:Ca and growth and

supported our conceptual model hypothesizing physiological-environmental controls on otolith chemistry. We found that within-individual correlations among physiologically regulated elements were generally stronger than those primarily controlled by environmental drivers. We also showed that failing to account for intrinsic effects resulted in inflated and biased estimates of among individual growth and element correlations.

Sources of intrinsic variation in element:Ca and growth

Age-related responses differed with each element:Ca and growth in ocean perch otoliths. The rate of element assimilation decreased as the fish aged for four of the five elements (except Sr:Ca), and growth rate also decreased with age, as is typical in most fish species. Age-related assimilation rates of elements should therefore be considered when reconstructing migratory histories, and as we have demonstrated, this is easily done through the use of univariate models that include age components as intrinsic effects to avoid the occurrence of age-dependent biases. Age-related responses are evident for many biogeochemical tracers and are quite valuable when aptly used. For example, to establish lifetime foraging patterns in avian species, stable isotope values in the blood and feathers of chicks are used to validate and interpret isotopic signatures found in immature and adult birds (Cherel and Hobson 2007, Cherel et al. 2014, Weimerskirch et al. 2014). Similarly, ontogenetic growth patterns in claws, hair, teeth, and bone of mammals allow stable isotopes or trace elements extracted from these tissues to be used to examine patterns of migration or foraging behavior (e.g. van der Merwe et al. 1990, Drucker et al. 2008, Ethier et al. 2014). Knowing metabolic turnover rates or deposition rates of tissues and the rate of integration of the biogeochemical tracer over an organism's life time are integral for framing ecological deductions within appropriate time scales (Ethier et al. 2010, Hobson et al. 2010, Ramos and González-Solís 2012).

Comparable *element:Ca - age* responses have been reported for other marine fish (Kalish 1989, Proctor et al. 1995, Hughes et al. 2015) with very different life history strategies, which suggests that these chemical patterns are a conserved and robust proxy for fish responses to changing ontogeny or environmental conditions. These species (i.e. blue grenadier (*Macruronus novaezelandiae*), Kalish 1989; Australian salmon (*Arripis trutta*), Hughes et al. 2015; and southern bluefin tuna (*Thunnus maccoyii*), Proctor et al. 1995) inhabit different marine environments (e.g. benthic/continental slope, coastal, or pelagic) and have varied reproductive strategies (e.g. heterochronal or isochronal spawners) compared to ocean perch (benthic/continental shelf and live-bearing) (e.g. Bruce et al. 2002).

Mg:Ca exhibited the least amount of synchrony between individuals through time. In marine fish, Mg in otoliths is not correlated with either temperature or salinity (as reviewed by Sturrock et al. 2012), but it is correlated with growth rate (Sturrock et al. 2015). Mg is required in many major metabolic pathways (Kaim et al. 2013), and the lack of observed synchrony could reflect individual metabolic processes and growth. Mg:Ca was most closely correlated (negatively) with the upwelling index; therefore, any changes in metabolic rates caused by the environmental fluctuations (e.g. temperature decreases, food resources change) could cause alterations in element assimilation rates. If Mg:Ca incorporation is as individualized as our data suggests, then we would expect the signal to be less synchronous and not correlate as strongly with growth or other elements. Further research and empirical data are needed define causal mechanisms.

Concentrations of Li:Ca and Ba:Ca showed moderate temporal synchrony compared to the other elements and also displayed seasonal, cyclic signals. Both Li:Ca and Ba:Ca tend to primarily correlate with environmental parameters as opposed to physiological processes, such as reproduction (e.g. Sturrock et al. 2012, Sturrock et al. 2015). However, Ba:Ca has been linked to diet (positive: Sanchez-Jerez et al. 2002, Buckel et al. 2004) and growth rate (negative: Miller 2011, Sturrock et al. 2015). Indeed, dietary sources have been shown to contribute up to 25% of otolith Ba in marine settings (Webb et al. 2012, Izzo et al. 2015).

Temporal patterns of element:Ca and growth displayed distinct seasonal trends. Na:Ca and Sr:Ca were the most consistent through time and had the highest individual synchrony among the element:Ca traits, but displayed an inverse relationship (i.e. Sr:Ca peaked in spring/summer; Na:Ca peaks in autumn/winter). Na is a physiologically important element (Kalish 1991, Thresher et al. 1994) and fluctuates not with the environment but with osmoregulatory control (Campana 1999). Seasonal sinusoidal patterns in otolith Sr:Ca over shorter time periods have been documented and are attributed to seasonal temperature changes aliased by reproductive physiology or other biological processes (Radtke and Targett 1984, Thorrold and Shuttleworth 2000, Hughes et al. 2015). Otolith Sr:Ca levels in plaice (*Pleuronectes platessa*) were highly correlated with physiological processes, particularly reproduction (Sturrock et al. 2015). Ocean perch are live-bearing (Pavlov and Emel'yanova 2013) and have a winter reproductive period with fertilization occurring in May/June, followed by gestation through the winter and parturition in October/November (Park 1993).

The timing of increases in otolith Sr:Ca corresponds with gestation and parturition, and it is possible the seasonal environmental signal (i.e. upwelling) aliases the underlying cause of Sr:Ca fluctuation in ocean perch otoliths. Additional research is required to conclusively define this relationship.

Environmental influences on element:Ca and growth

While age and individual variation accounted for most of the variability seen within the otolith trait profiles, some variation was attributed to environmental parameters. Seasonal upwelling is a key environmental driver of the local ecosystem, and we used this strong environmental signal to examine the otolith elemental composition and growth relationships experienced by a fully marine fish *in situ*. The upwelling process has a 'cascading' effect where multiple changes occur in the environment due to increased wind stress. As deeper water is brought to the surface, salinity and temperature change, and there is an influx of nutrients. The amount of change within the local environment is dependent on the characteristics of the water mass being upwelled in addition to the strength/duration of the wind driving the upwelling event (Bigg 2003). During an upwelling event within the Bonney upwelling system, both temperature and salinity decrease (e.g. temp: $\Delta \geq 4$°C; sal: 35.6 to 35.2‰) (Lewis 1981, Middleton and Bye 2007) and chlorophyll-a increases due to nutrient influx (Nieblas et al. 2009, van Ruth et al. 2010). All elements and growth, except Li:Ca, were correlated with the upwelling index as opposed to bottom temperature or chlorophyll-a. There were different directional relationships among the otolith traits with the upwelling index, and these persisted through time.

Otolith Ba:Ca was negatively related to the Bonney upwelling index and generally displayed maxima during autumn/winter and minima during spring/summer. The opposite relationship, a positive correlation, is seen in carbonate records from other upwelling systems (e.g. coral: Lea et al. 1989, Montaggioni et al. 2006; otoliths: Kingsford et al. 2009). In strong upwelling areas, usually dominated by large continental boundary currents or equatorial currents, waters tend to be Ba enriched due to dissolution of barite in deep ocean water and marine sediments (e.g. Lea and Boyle 1991, Shimmield 2015). Positive relationships between Ba:Ca concentrations of ambient water and those measured in fish otoliths have been well documented (as reviewed in Sturrock et al. 2012). Moreover, otolith Ba:Ca concentrations increase in as little as three days following increased levels of Ba:Ca in seawater (Wheeler et

al. 2016). Therefore, the otolith Ba:Ca profile found in the Bonney upwelling region may reflect reduced concentrations of Ba of the actual water mass being upwelled and alternative (non-upwelled) sources of greater Ba input into southern Australian marine waters during the autumn/winter months.

Source waters of the Flinders Current (the northern boundary current influencing the Bonney upwelling) are primarily Tasmanian Subantarctic Mode Water (TSAMW) formed in surface waters southwest of Tasmania at ≈ 47°S and subducted to depths of 400 to 800 m as it flows northwest (Barker 2004, Middleton and Bye 2007). Since the water mass transported by the Flinders Current and upwelled along the Bonney Coast has had very minimal contact with Ba enriched bottom waters/sediments, it may not produce a 'typical' positive Ba:Ca signal in the otoliths. In addition, while nutrient inputs and the productivity of the Bonney upwelling are well documented (e.g. Nieblas et al. 2009, van Ruth et al. 2010), sediment accumulation rates of biogenic compounds (including Ba) in the upwelling areas of Africa (Benguela Current) and South America (Peru Current) are 1 to 2 orders of magnitude higher compared to southern Australia (Veeh et al. 1999). Lower regional Ba sediment concentrations reflect the general oligotrophic nature of southern Australian waters. Alternative sources of Ba inputs may include wintertime strengthening of the eastward flowing Leeuwin Current (Middleton and Bye 2007), seasonal riverine inputs (Moore 1997, Sinclair and McCulloch 2004), and/or wintertime transport of coastal waters from the shelf to the deeper ocean (Kämpf et al. 2010).

Li:Ca in the otolith was most strongly correlated (positive) with chlorophyll-a levels in the environment as opposed to either the upwelling index (positive correlation) or bottom temperature (negative correlation). Interestingly, the negative relationship of otolith Li:Ca to water temperature has also been found in another fully marine fish, European plaice (*Pleuronectes platessa*) (Sturrock et al. 2015). In other biological carbonates, increased concentrations of Li:Ca link to changes in dissolved inorganic carbon (DIC) of seawater (foraminifera tests: Vigier et al. 2015) or to Li-rich phytoplankton diets (scallop shells: Thébault and Chauvaud 2013). Given this, otolith Li:Ca could be a potential indicator of productivity within the marine environment. Further, we recorded increased Li:Ca concentrations from the hyaline component of the otolith (i.e. summer growth; Paul and Horn 2009) as opposed to the opaque portion. Conversely, Li:Ca concentrations were positively correlated with opaque zones in plaice otoliths (Sturrock et al. 2015). This suggests that Li:Ca

631 is tied to environmental influences (e.g. temperature or primary productivity) rather than to
632 specific features of the otolith.
633
634 The addition of an age-environment interaction term allowed the response of the fish at a
635 given age to be examined from both the perspective of chemical assimilation in the otolith
636 and growth. Younger fish were more sensitive to upwelling and adjusted element assimilation
637 more rapidly to changing environmental conditions than older fish. For example, as
638 upwelling strengthened, the rate of Sr:Ca assimilation increased more quickly in younger fish
639 than older fish, while assimilation of Na:Ca decreased more rapidly. The best models for
640 Ba:Ca, Li:Ca and Mg:Ca did not include the age-environmental interaction term, indicating
641 that there was no difference in assimilation rates between younger and older fish. Whilst
642 overall there was a positive relationship between growth and upwelling, when explored
643 across ages, older fish grew proportionally better with increased upwelling. Younger fish
644 showed a negligible response. Because physical changes are happening at a rapid rate in an
645 upwelling system (e.g. drops in temperature/salinity, increased nutrients), metabolic
646 processes of a fish will adjust to cope (e.g. Brett and Groves 1979, Brown et al. 2004,
647 Wootton 2011). Resulting changes to metabolic processes could potentially cause rapid
648 adjustment of element assimilation rates, especially in elements under greater physiological
649 influence (e.g. Na and Sr). Fish within an upwelling environment will experience drops in
650 metabolic rates as temperature decreases, regulation of ionic homeostasis with changing
651 salinity, and increased water movement. Growth rates are influenced by changes to metabolic
652 processes caused by interactions of multiple environmental parameters, including changes to
653 food resources, relative to fish size and age (Brett and Groves 1979, Wootton 2011).
654
655 *Physiological versus environmental influences*
656 The multivariate modeling results corroborated our hypotheses regarding physiological
657 controls on elements in otoliths and present the first instance where correlations between
658 elements within individual otoliths and among fish have been determined (Figure 6a). Our
659 method provides 1) unbiased estimates of the strength and directionality of correlations, and
660 2) a clear methodological and statistical framework for future work. Within an individual
661 fish, Na:Ca and Sr:Ca were highly correlated with each other, and to a lesser extent, growth
662 and Mg:Ca, reflecting greater physiological influence (e.g. Thresher et al. 1994, Thorrold and
663 Shuttleworth 2000, Brown and Severin 2009, Sturrock et al. 2015). Ba:Ca and Li:Ca were
664 indeed less controlled by physiological processes and likely more reflective of extrinsic

influences based on the absence of a correlation with growth and weak correlations with Na:Ca and Sr:Ca. Mg:Ca correlated weakly to moderately with all otolith traits, corroborating that Mg:Ca in the otolith is regulated simultaneously by physiological and environmental factors. These findings support our hypotheses regarding otolith traits within an individual (Figure 1): 1) Na:Ca and Sr:Ca were predominantly influenced by an individual's physiology; 2) Ba:Ca and Li:Ca were primarily affected by environmental parameters; 3) growth rate and Mg:Ca were moderately influenced by both physiology and the environment; 4) correlations were stronger within groups of either physiologically or environmentally influenced otolith traits, but less so between the two groups; and 5) the strength of correlation varied among the otolith traits, particularly those under environmental control.

Element:Ca and growth were also compared among individuals, and surprisingly only Ba:Ca and growth were significantly correlated (negative). This means fish with overall higher growth rates equated to overall lower Ba:Ca. Given that upwelled water had lower Ba concentrations, but upwelling were times of higher average growth, a possible explanation is that fish whose lives spanned periods with stronger upwelling events would have elevated growth and reduced Ba; those inhabiting weaker upwelling periods would have the opposite. We hypothesized that otolith traits driven by environmental conditions would correlate both within an otolith, reflecting the time dependency of growth and element assimilation, and among individual fish that experience a similar set of external conditions (Figure 1). Our hypothesis is partially refuted since the only among-individual correlation was between Ba:Ca and growth. Therefore, the lack of among-individual correlations in other elements suggests that caution is needed when assuming multi-elemental signatures are reflective solely of shared environments. These results potentially have major implications for the use of biogeochemical proxies in a range of fish ecology studies.

Ignoring intrinsic effects in the multivariate mixed model resulted in elevated estimates of among individual element and growth correlations (Figure 6c). These results are biased because fish of similar ages have similar overall elemental concentrations due to intrinsic processes, rather than any shared environmental conditions. For example, Sr:Ca ratios decrease with increased growth during metamorphosis in Japanese eels (*Anguilla japonica*; Arai et al. 1997), and seasonal variations of Sr and Na in otoliths are linked to changes in growth rates or reproductive investment rather than shared environmental conditions (Kalish 1989, 1991). The qualitatively similar within individual correlations from both models are

699 expected because comparisons are made on the same scale (i.e. among measurements made at
700 the same otolith location).
701
702 *Conclusions*
703 The application of univariate and multivariate mixed-effects modeling to time resolved
704 element:Ca and growth profiles has provided a novel method to disentangle the effects of
705 physiology and the environment on otolith chemistry and fish growth. If changes to element
706 concentrations in otoliths driven by physiology are unaccounted for (e.g. age, reproductive
707 parameters, diet), then elemental data used to reconstruct lifetime movements or as
708 paleoproxies can be misinterpreted (Thresher 1999, Elsdon et al. 2008, Sturrock et al. 2012).
709 Our models accounted for age-related effects but did not include reproductive parameters or
710 diet as these data were unavailable. However, since both male and female fish were included
711 in the models, the element:Ca profiles and growth are integrated to reflect the response of all
712 fish, regardless of sex. The Sr:Ca temporal signal and its association with reproduction
713 should be explored, as this relationship has potential for use as a proxy to reconstruct
714 reproductive histories. This would be especially useful when examining exploited
715 populations for changes in reproductive characteristics through time, i.e. changes in age-at-
716 maturity, shifts in spawning season with climate variability. Since both Ba:Ca and Li:Ca were
717 under limited physiological control, these elements are the most likely candidates for use as
718 environmental proxies. Otolith Li:Ca is particularly promising as an indicator of productivity
719 in the marine environment given its positive correlation with chlorophyll-a. Describing the
720 assimilation mechanism of Li from the environment into the otolith will be an important first
721 step. In a similar vein, Ba:Ca seems to track presumed Ba concentrations within the ambient
722 water mass, if the Bonney upwelled water does indeed reflect a non-enriched Ba source. Of
723 all the elements examined, Ba was the only one that was correlated among individuals, which
724 suggests that population-level fluctuations in ambient Ba are simultaneously recorded by all
725 individuals. Therefore, fluctuations in Ba:Ca are likely to represent broad-scale
726 environmental change as opposed to individual-based differences in assimilation. Further
727 research directions should include quantifying physiological (e.g. metabolism, reproductive
728 condition) and environmental influences on element assimilation by focusing on all life
729 history stages, since element assimilation is inherently linked with age-based growth. Related
730 to this point is the need for the collection of targeted empirical data and detailed sensitivity
731 analyses to assess how temporal and spatial variation in ambient elemental concentrations
732 interacts with age-dependent assimilation.

Acknowledgements:

We acknowledge partial funding from the Dr Paris Goodsell Marine Ecology Research Grant, the Nature Foundation SA, the Ecological Society of Australia, CSIRO Wealth from Oceans Flagship and the Australian Research Council (FT100100767 and DP110100716 awarded to BMG). We acknowledge Aoife McFadden and Benjamin Wade of Adelaide Microscopy for assistance with LA ICP-MS. Special thanks to Joel Redman and Scott Redman of Southend, SA for help with specimen collection. G. L. Grammer was supported by a CSIRO Wealth from Oceans Flagship Postgraduate Scholarship and an Adelaide Scholarship International (University of Adelaide).

Literature Cited:

Arai, T., T. Otake, and K. Tsukamoto. 1997. Drastic changes in otolith microstructure and microchemistry accompanying the onset of metamorphosis in the Japanese eel *Anguilla japonica*. Marine Ecology Progress Series **161**:17-22.

Batenburg, S. J., G.-J. Reichart, T. Jilbert, M. Janse, F. P. Wesselingh, and W. Renema. 2011. Interannual climate variability in the Miocene: High resolution trace element and stable isotope ratios in giant clams. Palaeogeography, Palaeoclimatology, Palaeoecology **306**:75-81.

Bates, D., M. Maechler, B. Bolker, and S. Walker. 2014. lme4: Linear mixed-effects models using Eigen and S4. R package version 1.1-7. http://cran.r-project.org/web/packages/lme4/.

Botsford, L. W., C. A. Lawrence, E. P. Dever, A. Hastings, and J. Largier. 2003. Wind strength and biological productivity in upwelling systems: an idealized study. Fisheries Oceanography **12**:245-259.

Brett, J. R., and T. D. D. Groves. 1979. Physiological energetics. Pages 279-352 *in* W. S. Hoar, D. J. Randall, and J. R. Brett, editors. Fish Physiology: Bioenergetics and Growth. Academic Press, London.

Brown, J. H., J. F. Gillooly, A. P. Allen, V. M. Savage, and G. B. West. 2004. Toward a metabolic theory of ecology. Ecology **85**:1771-1789.

Brown, R. J., and K. P. Severin. 2009. Otolith chemistry analyses indicate that water Sr:Ca is the primary factor influencing otolith Sr:Ca for freshwater and diadromous fish but not for marine fish. Canadian Journal of Fisheries and Aquatic Sciences **66**:1790-1808.

765 Bruce, B. D., R. Bradford, R. Daley, M. Green, and K. Phillips. 2002. Targeted review of
766 biological and ecological information from fisheries research in the South East Marine
767 Region National Oceans Office, CSIRO Marine Research, Hobart:175.
768 Buckel, J. A., B. L. Sharack, and V. S. Zdanowicz. 2004. Effect of diet on otolith
769 composition in *Pomatomus saltatrix*, an estuarine piscivore. Journal of Fish Biology
770 **64**:1469-1484.
771 Bulman, C., F. Althaus, X. He, N. Bax, and A. Williams. 2001. Diets and trophic guilds of
772 demersal fishes of the south-eastern Australian shelf. Marine and Freshwater Research
773 **52**:537-548.
774 Burnham, K. P., and D. R. Anderson. 2004. Multimodel inference: understanding AIC and
775 BIC in model selection. Sociological Methods & Research **33**:261-304.
776 Campana, S. E. 1999. Chemistry and composition of fish otoliths: pathways, mechanisms and
777 applications. Marine Ecology Progress Series **188**:263-297.
778 Cherel, Y., and K. A. Hobson. 2007. Geographical variation in carbon stable isotope
779 signatures of marine predators: a tool to investigate their foraging areas in the Southern
780 Ocean. Marine Ecology Progress Series **329**:281-287.
781 Cherel, Y., S. Jaquemet, A. Maglio, and A. Jaeger. 2014. Differences in δ13C and δ15N
782 values between feathers and blood of seabird chicks: implications for non-invasive
783 isotopic investigations. Marine Biology **161**:229-237.
784 Cresson, P., M. Bouchoucha, F. Morat, F. Miralles, F. Chavanon, V. Loizeau, and D. Cossa.
785 2015. A multitracer approach to assess the spatial contamination pattern of hake
786 (*Merluccius merluccius*) in the French Mediterranean. Science of the Total Environment
787 **532**:184-194.
788 Cusack, M., and A. Freer. 2008. Biomineralization: elemental and organic influence in
789 carbonate systems. Chemical Reviews **108**:4433-4454.
790 de Vries, M. C., B. M. Gillanders, and T. S. Elsdon. 2005. Facilitation of barium uptake into
791 fish otoliths: Influence of strontium concentration and salinity. Geochimica et
792 Cosmochimica Acta **69**:4061-4072.
793 Dingemanse, N. J., and N. A. Dochtermann. 2013. Quantifying individual variation in
794 behaviour: mixed-effect modelling approaches. Journal of Animal Ecology **82**:39-54.
795 Disspain, M., L. A. Wallis, and B. M. Gillanders. 2011. Developing baseline data to
796 understand environmental change: a geochemical study of archaeological otoliths from
797 the Coorong, South Australia. Journal of Archaeological Science **38**:1842-1857.

798 Disspain, M. C. F., S. Ulm, and B. M. Gillanders. 2015. Otoliths in archaeology: methods,
799 applications and future prospects. Journal of Archaeological Science: Reports.
800 Drucker, D. G., A. Bridault, K. A. Hobson, E. Szuma, and H. Bocherens. 2008. Can carbon-
801 13 in large herbivores reflect the canopy effect in temperate and boreal ecosystems?
802 Evidence from modern and ancient ungulates. Palaeogeography, Palaeoclimatology,
803 Palaeoecology **266**:69-82.
804 Elsdon, T. S., and B. M. Gillanders. 2002. Interactive effects of temperature and salinity on
805 otolith chemistry: challenges for determining environmental histories of fish. Canadian
806 Journal of Fisheries and Aquatic Sciences **59**:1796-1808.
807 Elsdon, T. S., and B. M. Gillanders. 2003a. Reconstructing migratory patterns of fish based
808 on environmental influences on otolith chemistry. Reviews in Fish Biology and Fisheries
809 **13**:217-235.
810 Elsdon, T. S., and B. M. Gillanders. 2003b. Relationship between water and otolith elemental
811 concentrations in juvenile black bream *Acanthopagrus butcheri*. Marine Ecology
812 Progress Series **260**:263-272.
813 Elsdon, T. S., and B. M. Gillanders. 2005. Consistency of patterns between laboratory
814 experiments and field collected fish in otolith chemistry: an example and applications for
815 salinity reconstructions. Marine and Freshwater Research **56**:609-617.
816 Elsdon, T. S., B. K. Wells, S. E. Campana, B. M. Gillanders, C. M. Jones, K. E. Limburg, D.
817 H. Secor, S. R. Thorrold, and B. D. Walther. 2008. Otolith chemistry to describe
818 movements and life-history parameters of fishes: Hypotheses, assumptions, limitations
819 and inferences. Pages 297-+ *in* R. N. Gibson, R. J. A. Atkinson, and J. D. M. Gordon,
820 editors. Oceanography and Marine Biology: An Annual Review, Vol 46. Crc Press-
821 Taylor & Francis Group, Boca Raton.
822 Ethier, D. M., C. J. Kyle, T. K. Kyser, and J. J. Nocera. 2010. Variability in the growth
823 patterns of the cornified claw sheath among vertebrates: implications for using
824 biogeochemistry to study animal movement. Canadian Journal of Zoology **88**:1043-
825 1051.
826 Ethier, D. M., C. J. Kyle, and J. J. Nocera. 2014. Tracking animal movement by comparing
827 trace element signatures in claws to spatial variability of elements in soils. Science of the
828 Total Environment **468–469**:699-705.
829 Fox, J., S. Weisberg, and J. Hong. 2014. effects: Effect displays for linear, generalized linear,
830 and other models. R package version 3.0-3. http://cran.r-
831 project.org/web/packages/effects/index.html.

832 Gillanders, B. M. 2002. Temporal and spatial variability in elemental composition of otoliths:
833 Implications for determining stock identity and connectivity of populations. Canadian
834 Journal of Fisheries and Aquatic Sciences **59**:669-679.
835 Griffin, W. L., W. J. Powell, N. J. Pearson, and S. Y. O'Reilly. 2008. GLITTER: data
836 reduction software for laser ablation ICP-MS. Pages 204-207 *in* P. Sylvester, editor.
837 Laser Ablation: ICP-MS in the Earth Sciences Mineralogical Association of Canada
838 Short Course Series.
839 Hadfield, J. D. 2010. MCMC methods for multi-response generalised linear mixed models:
840 the MCMCglmm R package. Journal of Statistical Software **33**:1-22.
841 Hadfield, J. D., A. J. Wilson, D. Garant, B. C. Sheldon, and L. E. B. Kruuk. 2010. The
842 misuse of BLUP in ecology and evolution. American Naturalist **175**:116-125.
843 Harrell, F. E. J. 2014. Hmisc: Harrell Miscellaneous. R package version 3.14-5. http://cran.r-
844 project.org/web/packages/Hmisc/.
845 Hatch, M. B. A., S. A. Schellenberg, and M. L. Carter. 2013. Ba/Ca variations in the modern
846 intertidal bean clam *Donax gouldii*: An upwelling proxy? Palaeogeography,
847 Palaeoclimatology, Palaeoecology **373**:98-107.
848 Henschke, N., D. A. Bowden, J. D. Everett, S. P. Holmes, R. J. Kloser, R. W. Lee, and I. M.
849 Suthers. 2013. Salp-falls in the Tasman Sea: a major food input to deep-sea benthos.
850 Marine Ecology Progress Series **491**:165-175.
851 Hobson, K. A., R. Barnett-Johnson, and T. Cerling. 2010. Using Isoscapes to Track Animal
852 Migration. Pages 273-298 *in* B. J. West, J. G. Bowen, E. T. Dawson, and P. K. Tu,
853 editors. Isoscapes: Understanding movement, pattern, and process on Earth through
854 isotope mapping. Springer Netherlands, Dordrecht.
855 Horn, P. L., J. S. Forman, and M. R. Dunn. 2012. Dietary partitioning by two sympatric fish
856 species, red cod (*Pseudophycis bachus*) and sea perch (*Helicolenus percoides*), on
857 Chatham Rise, New Zealand. Marine Biology Research **8**:624-634.
858 Hughes, J. M., J. Stewart, B. M. Gillanders, D. Collins, and I. M. Suthers. 2015. Relationship
859 between otolith chemistry and age in a widespread pelagic teleost *Arripis trutta*:
860 influence of adult movements on stock structure and implications for management.
861 Marine and Freshwater Research **67**:224-237.
862 Izzo, C., Z. A. Doubleday, G. L. Grammer, M. Disspain, Q. Ye, and B. M. Gillanders. 2016.
863 Seasonally resolved environmental reconstructions using fish otoliths. Canadian Journal
864 of Fisheries and Aquatic Sciences. DOI: 10.1139/cjfas-2016-0055.

Izzo, C., Z. A. Doubleday, A. G. Schultz, S. H. Woodcock, and B. M. Gillanders. 2015. Contribution of water chemistry and fish condition to otolith chemistry: comparisons across salinity environments. Journal of Fish Biology **86**:1680-1698.

James, N. P., and Y. Bone. 2011. Neritic Carbonate Sediments in a Temperate Realm: Southern Australia. Springer, London.

Johnson, P. C. D. 2014. Extension of Nakagawa & Schielzeth's R2GLMM to random slopes models. Methods in Ecology and Evolution **5**:944-946.

Kaim, W., B. Schwederski, and A. Klein. 2013. Bioinorganic Chemistry--Inorganic Elements in the Chemistry of Life: An Introduction and Guide. 2nd edition. John Wiley & Sons, United Kingdom.

Kalish, J. M. 1989. Otolith microchemistry: validation of the effects of physiology, age and environment on otolith composition. Journal of Experimental Marine Biology and Ecology **132**:151-178.

Kalish, J. M. 1991. Determinants of otolith chemistry: seasonal variation in the composition of blood plasma, endolymph and otoliths of bearded rock cod *Pseudophycis barbatus*. Marine Ecology Progress Series **74**:137-159.

Kämpf, J., M. Doubell, D. Griffin, R. L. Matthews, and T. M. Ward. 2004. Evidence of a large seasonal coastal upwelling system along the southern shelf of Australia. Geophysical Research Letters **31**.

Kämpf, J., N. Payne, and P. Malthouse. 2010. Marine connectivity in a large inverse estuary. Journal of Coastal Research **26**:1047-1056.

Kingsford, M. J., J. M. Hughes, and H. M. Patterson. 2009. Otolith chemistry of the non-dispersing reef fish *Acanthochromis polyacanthus*: cross-shelf patterns from the central Great Barrier Reef. Marine Ecology Progress Series **377**:279-288.

Lea, D. W., and E. A. Boyle. 1991. Barium in planktonic foraminifera. Geochimica et Cosmochimica Acta **55**:3321-3331.

Lea, D. W., G. T. Shen, and E. A. Boyle. 1989. Coralline barium records temporal variability in equatorial pacific upwelling. Nature **340**:373-373.

Lewis, R. 1981. Seasonal upwelling along the south-eastern coastline of South Australia. Marine and Freshwater Research **32**:843-854.

Mazerolle, M. J. 2015. Model selection and multimodel inference based on (Q)AIC(c). R package version 2.0-3. http://cran.r-project.org/web/packages/AICcmodavg/index.html.

Middleton, J. F., and J. A. T. Bye. 2007. A review of the shelf-slope circulation along Australia's southern shelves: Cape Leeuwin to Portland. Progress in Oceanography **75**:1-41.

Middleton, J. F., and M. Cirano. 2002. A northern boundary current along Australia's southern shelves: The Flinders Current. Journal of Geophysical Research. C. Oceans **107**:1-11.

Middleton, J. F., R. McGarvey, A. Linnane, S. M. Middleton, C. E. P. Teixeira, and P. Hawthorne. 2012. Using observations of bottom temperature to calibrate the output of an ocean model. Journal of Marine Systems **91**:34-40.

Miller, J. A. 2011. Effects of water temperature and barium concentration on otolith composition along a salinity gradient: Implications for migratory reconstructions. Journal of Experimental Marine Biology and Ecology **405**:42-52.

Montaggioni, L. F., F. Le Cornec, T. Correge, and G. Cabioch. 2006. Coral barium/calcium record of mid-Holocene upwelling activity in New Caledonia, South-West Pacific. Palaeogeography, Palaeoclimatology, Palaeoecology **237**:436-455.

Moore, W. S. 1997. High fluxes of radium and barium from the mouth of the Ganges-Brahmaputra River during low river discharge suggest a large groundwater source. Earth and Planetary Science Letters **150**:141-150.

Morrongiello, J. R., and R. E. Thresher. 2015. A statistical framework to explore ontogenetic growth variation among individuals and populations: a marine fish example. Ecological Monographs **85**:93-115.

Morrongiello, J. R., C. T. Walsh, C. A. Gray, J. R. Stocks, and D. A. Crook. 2014. Environmental change drives long-term recruitment and growth variation in an estuarine fish. Global Change Biology **20**:1844-1860.

Nakagawa, S., and H. Schielzeth. 2013. A general and simple method for obtaining R^2 from generalized linear mixed-effects models. Methods in Ecology and Evolution **4**:133-142.

Nieblas, A. E., B. M. Sloyan, A. J. Hobday, R. Coleman, and A. J. Richardson. 2009. Variability of biological production in low wind-forced regional upwelling systems: A case study off southeastern Australia. Limnology and Oceanography **54**:1548-1558.

Park, T. J. 1993. A comparison of the morphology, growth and reproductive biology of two colour forms of ocean perch (*Helicoleus percoides*), NSW, Australia. Masters. University of Sydney, Sydney, Australia.

Parrish, J. R., D. T. Rogers, and F. P. Ward. 1983. Identification of natal locales of peregrine falcons (*Falco peregrinus*) by trace-element analysis of feathers. The Auk **100**:560-567.

931 Paul, L. J., and P. L. Horn. 2009. Age and growth of sea perch (*Helicolenus percoides*) from
932 two adjacent areas off the east coast of South Island, New Zealand. Fisheries Research
933 **95**:169-180.
934 Pavlov, D. A., and N. G. Emel'yanova. 2013. Transition to viviparity in the order
935 Scorpaeniformes: Brief review. Journal of Ichthyology **53**:52-69.
936 Proctor, C. H., R. E. Thresher, J. S. Gunn, D. J. Mills, I. R. Harrowfield, and S. H. Sie. 1995.
937 Stock structure of the southern bluefin tuna *Thunnus maccoyii:* an investigation based on
938 probe microanalysis of otolith composition. Marine Biology **122**:511-526.
939 Radtke, R. L., and T. E. Targett. 1984. Rhythmic structural and chemical patterns in otoliths
940 of the Antarctic fish *Notothenia larseni*: Their application to age determination. Polar
941 Biology **3**:203-210.
942 Ramos, R., and J. González-Solís. 2012. Trace me if you can: the use of intrinsic
943 biogeochemical markers in marine top predators. Frontiers in Ecology and the
944 Environment **10**:258-266.
945 Reis-Santos, P., S. E. Tanner, R. P. Vasconcelos, T. S. Elsdon, H. N. Cabral, and B. M.
946 Gillanders. 2013. Connectivity between estuarine and coastal fish populations:
947 contributions of estuaries are not consistent over time. Marine Ecology Progress Series
948 **491**:177-186.
949 Rubenstein, D. R., and K. A. Hobson. 2004. From birds to butterflies: animal movement
950 patterns and stable isotopes. Trends in Ecology & Evolution **19**:256-263.
951 Sanchez-Jerez, P., B. M. Gillanders, and M. J. Kingsford. 2002. Spatial variability of trace
952 elements in fish otoliths: comparison with dietary items and habitat constituents in
953 seagrass meadows. Journal of Fish Biology **61**:801-821.
954 Shimmield, G. 2015. Biogenic barium. Pages 1-2 *in* J. Harff, M. Meschede, S. Petersen, and
955 J. Thiede, editors. Encyclopedia of Marine Geosciences. Springer Netherlands.
956 Sinclair, D. J., and M. T. McCulloch. 2004. Corals record low mobile barium concentrations
957 in the Burdekin River during the 1974 flood: evidence for limited Ba supply to rivers?
958 Palaeogeography, Palaeoclimatology, Palaeoecology **214**:155-174.
959 Smith, P. J., C. D. Struthers, C. D. Paulin, S. M. McVeagh, and R. K. Daley. 2009. Shallow
960 genetic and morphological divergence among seaperches in the South Pacific (family
961 Scorpaenidae; genus *Helicolenus*). Journal of Fish Biology **74**:1104-1128.
962 Stanley, S. M. 2006. Influence of seawater chemistry on biomineralization throughout
963 phanerozoic time: Paleontological and experimental evidence. Palaeogeography,
964 Palaeoclimatology, Palaeoecology **232**:214-236.

965 Sturrock, A. M., E. Hunter, J. A. Milton, E. Eimf, R. C. Johnson, C. P. Waring, and C. N.
966 Trueman. 2015. Quantifying physiological influences on otolith microchemistry.
967 Methods in Ecology and Evolution **6**:806-816.
968 Sturrock, A. M., C. N. Trueman, A. M. Darnaude, and E. Hunter. 2012. Can otolith elemental
969 chemistry retrospectively track migrations in fully marine fishes? Journal of Fish
970 Biology **81**:766-795.
971 Sturrock, A. M., C. N. Trueman, J. A. Milton, C. P. Waring, M. J. Cooper, and E. Hunter.
972 2014. Physiological influences can outweigh environmental signals in otolith
973 microchemistry research. Marine Ecology Progress Series **500**:245-264.
974 Thébault, J., and L. Chauvaud. 2013. Li/Ca enrichments in great scallop shells (*Pecten*
975 *maximus*) and their relationship with phytoplankton blooms. Palaeogeography,
976 Palaeoclimatology, Palaeoecology **373**:108-122.
977 Thorrold, S. R., and S. Shuttleworth. 2000. In situ analysis of trace elements and isotope
978 ratios in fish otoliths using laser ablation sector field inductively coupled plasma mass
979 spectrometry. Canadian Journal of Fisheries and Aquatic Sciences **57**:1232-1242.
980 Thresher, R. E. 1999. Elemental composition of otoliths as a stock delineator in fishes.
981 Fisheries Research **43**:165-204.
982 Thresher, R. E., C. H. Proctor, J. S. Gunn, and I. R. Harrowfield. 1994. An evaluation of
983 electron-probe microanalysis of otoliths for stock delineation and identification of
984 nursery areas in a southern temperate groundfish, *Nemadactylus macropterus*
985 (Cheilodactylidae). Fishery Bulletin **92**:817-840.
986 van der Merwe, N. J., J. A. Lee-Thorp, J. F. Thackeray, A. Hall-Martin, F. J. Kruger, H.
987 Coetzee, R. H. V. Bell, and M. Lindeque. 1990. Source-area determination of elephant
988 ivory by isotopic analysis. Nature **346**:744-746.
989 van Ruth, P. D., G. G. Ganf, and T. M. Ward. 2010. Hot-spots of primary productivity: an
990 alternative interpretation to conventional upwelling models. Estuarine, Coastal and Shelf
991 Science **90**:142-158.
992 Veeh, H. H., D. T. Heggie, and A. J. Crispe. 1999. Biogeochemistry of southern Australian
993 continental slope sediments. Australian Journal of Earth Sciences **46**:563-575.
994 Vigier, N., C. Rollion-Bard, Y. Levenson, and J. Erez. 2015. Lithium isotopes in foraminifera
995 shells as a novel proxy for the ocean dissolved inorganic carbon (DIC). Comptes Rendus
996 Geoscience **347**:43-51.

997 Walther, B., M. Kingsford, M. O'Callaghan, and M. McCulloch. 2010. Interactive effects of
998 ontogeny, food ration and temperature on elemental incorporation in otoliths of a coral
999 reef fish. Environmental Biology of Fishes **89**:441-451.
1000 Walther, B. D., M. J. Kingsford, and M. T. McCulloch. 2013. Environmental records from
1001 Great Barrier Reef corals: inshore versus offshore drivers. PLoS ONE **8**:e77091.
1002 Webb, S. D., S. H. Woodcock, and B. M. Gillanders. 2012. Sources of otolith barium and
1003 strontium in estuarine fish and the influence of salinity and temperature. Marine Ecology
1004 Progress Series **453**:189-199.
1005 Weimerskirch, H., Y. Cherel, K. Delord, A. Jaeger, S. C. Patrick, and L. Riotte-Lambert.
1006 2014. Lifetime foraging patterns of the wandering albatross: Life on the move! Journal of
1007 Experimental Marine Biology and Ecology **450**:68-78.
1008 Weiner, S., and P. M. Dove. 2003. An overview of biomineralization processes and the
1009 problem of the vital effect. Reviews in Mineralogy and Geochemistry **54**:1-29.
1010 Weisberg, S., G. Spangler, and L. S. Richmond. 2010. Mixed effects models for fish growth.
1011 Canadian Journal of Fisheries & Aquatic Sciences **67**:269-277.
1012 Wheeler, S. G., A. D. Russell, J. S. Fehrenbacher, and S. G. Morgan. 2016. Evaluating
1013 chemical signatures in a coastal upwelling region to reconstruct water mass associations
1014 of settlement-stage rockfishes. Marine Ecology Progress Series **550**:191-206.
1015 Woodson, L. E., B. K. Wells, C. B. Grimes, R. P. Franks, J. A. Santora, and M. H. Carr.
1016 2013. Water and otolith chemistry identify exposure of juvenile rockfish to upwelled
1017 waters in an open coastal system. Marine Ecology Progress Series **473**:261-273.
1018 Wootton, R. J. 2011. Energy utilization in growth | Growth: environmental effects. Pages
1019 1629-1635 *in* A. P. Farrell, editor. Encyclopedia of Fish Physiology. Academic Press,
1020 San Diego.
1021 Zuur, A., E. N. Ieno, N. Walker, A. A. Saveliev, and G. M. Smith. 2009. Mixed effects
1022 models and extensions in ecology with R. Springer, New York.
1023
1024
1025 **Data Availability:**
1026 Data associated with this paper are available in the Dryad Digital Repository:
1027 http://dx.doi.org/10.5061/dryad.cn55b
1028

Tables:

Table 1. Description of fixed (intrinsic and extrinsic) and random effects used in the analyses of trace elements and growth derived from the otoliths of ocean perch.

Variable	Description	Data Range
Intrinsic Fixed effects		
Age	Age when each monthly increment was formed.	14 - 85 mo (1.2 - 7.1 yrs)
age.month.cap	Age of the fish in months at date of capture	37 - 223 mo (3.1 - 18.6 yrs)
Random Effects		
FishID	Unique identifier for each fish	n = 38
Month	A code designating the specific month and year of each monthly resolved increment (i.e. 75 = Dec 1996, 76 = Jan 1997, etc.)	204 mo (17 yrs) (Nov 1995 - Oct 2012)
Extrinsic Fixed effects		
Bonney UI	Monthly NOAA PFEL Global 1-degree Upwelling Index calculated for the Bonney Coast region of South Australia (37.6°S, 139.8°E; coast angle: 144°) *Source: http://www.pfeg.noaa.gov/products/las/docs/global_upwell.html*	1981 - 2014
Bottom Temp	Corrected monthly Bluelink bottom temperature (°C) derived in Middleton et al. (2012) and extended with bottom temperature logger data from Southend, SA	1993 - 2013

Chl-a	MODIS Aqua Level 3 Global Monthly Mapped 4 km Chlorophyll a ($mg \cdot m^{-3}$) for the Bonney Coast, SA (37°S, 139°E) *Source: http://thredds.jpl.nasa.gov/las/getUI.do*	2002 - 2013

1032

1033 Table 2. Best random effect structure fitted with the full fixed effect structure of *Age* +
1034 *age.month.cap* for each element:Ca and growth.
1035

Model	df	AICc	ΔAICc	LL
Ba:Ca				
FishID	5	-1034.60	561.11	522.31
Age|FishID	7	-1470.50	125.21	742.27
Age|FishID + Month	8	-1513.44	82.27	764.75
Age|FishID + Age|Month	**10**	**-1595.71**	**0.00**	**807.90**
Na:Ca				
FishID	5	-6180.57	483.68	3095.30
Age|FishID	7	-6419.22	245.03	3216.64
Age|FishID + Month	8	-6660.21	4.05	3338.13
Age|FishID + Age|Month	**10**	**-6664.25**	**0.00**	**3342.17**
Sr:Ca				
FishID	5	-5681.03	462.22	2845.53
Age|FishID	7	-5997.87	145.38	3005.96
Age|FishID + Month	8	-6116.31	26.94	3066.18
Age|FishID + Age|Month	**10**	**-6143.25**	**0.00**	**3081.67**
Mg:Ca				
FishID	5	-2025.91	323.48	1017.97
Age|FishID	7	-2291.68	57.71	1152.87
Age|FishID + Month	8	-2321.44	27.96	1168.75
Age|FishID + Age|Month	**10**	**-2349.39**	**0.00**	**1184.75**
Li:Ca				
FishID	5	1889.82	813.49	-939.90
Age|FishID	7	1225.35	149.01	-605.65
Age|FishID + Month	8	1135.86	59.52	-559.90
Age|FishID + Age|Month	**10**	**1076.34**	**0.00**	**-528.12**
Growth				

FishID	5	-696.97	1099.24	353.50
Age|FishID	7	-1182.57	613.64	598.31
Age|FishID + Month	8	-1568.77	227.45	792.41
Age|FishID + Age|Month	**10**	**-1796.22**	**0.00**	**908.15**

Notes: Best random effect structure is highlighted in **bold.** Best model rankings were assessed using Akaike's information criterion corrected for small sample sizes (AICc). LL: Log Likelihood. Random slope term designated with A|B.

1040 Table 3. Variance components, parameter estimates and test statistics for the optimal model of each
1041 element:Ca and growth.
1042

Statistic	Random effect					Fixed effect		
	FishID	Age|FishID	Month	Age|Month	Residual	Intercept	Age	Age.month.cap
Mg:Ca								
Variance	0.026	0.015	0.001	0.004	0.017			
SD	0.160	0.122	0.032	0.060	0.131			
Corr.		0.300		−0.890				
Estimate						3.903	−0.188	…
SE						0.027	0.022	…
t						142.70	−8.390	…
Li:Ca								
Variance	0.077	0.197	0.008	0.026	0.076			
SD	0.277	0.443	0.088	0.160	0.275			
Corr.		0.200		−0.810				
Estimate						2.212	−0.344	−0.002
SE						0.046	0.075	0.001
t						47.830	−4.550	−2.650
Ba:Ca								
Variance	0.020	0.033	0.002	0.010	0.024			
SD	0.142	0.180	0.048	0.100	0.155			
Corr.		0.220		−0.800				
Estimate						0.492	−0.187	0.001
SE						0.024	0.032	0.000
t						20.491	−5.830	1.684
Na:Ca								
Variance	0.005	0.003	0.001	0.000	0.003			
SD	0.074	0.053	0.026	0.008	0.053			
Corr.		0.470		−1.000				
Estimate						9.338	−0.189	…
SE						0.012	0.009	…
t						754.100	−20.400	…
Sr:Ca								
Variance	0.002	0.005	0.001	0.001	0.004			
SD	0.047	0.068	0.024	0.022	0.060			

Corr.		0.330		−0.840				
Estimate						8.082	0.143	0.000
SE						0.008	0.012	0.000
t						991.400	12.100	2.300
Growth								
Variance	0.032	0.060	0.008	0.019	0.020			
SD	0.178	0.245	0.091	0.138	0.140			
Corr.		0.310		0.710				
Estimate						2.137	−0.883	…
SE						0.030	0.042	…
t						71.570	−20.930	…

Notes: Intraclass correlation coefficients (ICC) of the six otolith traits for *Month* are: Mg:Ca, 1.74; Li:Ca, 3.30; Growth, 8.50; Ba:Ca, 2.05; Na:Ca, 5.08; Sr:Ca, 5.02. Optimal models were fitted using restricted maximum likelihood (REML). Random slope term designated with A|B.

1047 Table 4. Model selection for environmental variables fitted to each optimal model.

Response Variable	Environmental Variables	df	AICc	ΔAICc	Log Likelihood	R^2m	R^2c	Estimate	±SE	t-statistic
Ba:Ca	+ Growth	10	-1620.3	4.7	820.2	0.127	0.626			
	+ Bonney UI	**11**	**-1625.0**	**0.0**	**823.5**	**0.128**	**0.626**	**-0.0002**	**0.0001**	**-2.616**
	+ Bottom Temp	11	-1618.7	6.3	820.4	0.127	0.627			
	+ Chl-a	11	-1047.0	577.9	534.6	0.123	0.603			
	*+ Age * Bonney UI*	*12*	*-1623.4*	*1.5*	*823.8*	*0.128*	*0.626*	*0.0001*	*0.0002*	*0.710*
	+ Age * Bottom Temp	12	-1619.4	5.5	821.8	0.128	0.627			
	+ Age * Chl-a	12	-1045.2	579.7	534.7	0.123	0.603			
Na:Ca	+ Growth	9	-6696.2	95.0	3357.1	0.461	0.842			
	+ Bonney UI	*10*	*-6778.9*	*12.3*	*3399.5*	*0.469*	*0.839*	*-0.0003*	*0.0000*	*-10.600*
	+ Bottom Temp	10	-6720.4	70.8	3370.2	0.464	0.840			
	+ Chl-a	10	-4111.2	2680.0	2065.7	0.443	0.839			
	+ Age * Bonney UI	**11**	**-6791.2**	**0.0**	**3406.7**	**0.470**	**0.839**	**0.0001**	**0.0000**	**3.800**
	+ Age * Bottom Temp	11	-6724.7	66.5	3373.4	0.465	0.840			
	+ Age * Chl-a	11	-4113.4	2677.8	2067.8	0.444	0.840			
Sr:Ca	+ Growth	10	-6174.2	75.5	3097.1	0.416	0.724			
	+ Bonney UI	*11*	*-6225.4*	*24.3*	*3123.7*	*0.438*	*0.719*	*0.0002*	*0.0000*	*8.600*
	+ Bottom Temp	11	-6197.8	51.9	3110.0	0.425	0.721			
	+ Chl-a	11	-3851.3	2398.4	1936.7	0.383	0.740			
	+ Age * Bonney UI	**12**	**-6249.7**	**0.0**	**3136.9**	**0.440**	**0.717**	**-0.0003**	**0.0000**	**-5.400**
	+ Age * Bottom Temp	12	-6199.0	50.6	3111.6	0.426	0.721			
	+ Age * Chl-a	12	-3854.6	2395.1	1939.4	0.385	0.739			

1048

1049 Table 4. Extended.

Response Variable	Environmental Variables	df	AICc	ΔAICc	Log Likelihood	R^2m	R^2c	Estimate	±SE	t-statistic
Mg:Ca	+ Growth	9	-2376.1	16.9	1197.1	0.145	0.695			
	+ Bonney UI	**10**	**-2393.0**	**0.0**	**1206.6**	**0.147**	**0.695**	**-0.0002**	**0.0000**	**-4.430**
	+ Bottom Temp	10	-2375.6	17.4	1197.9	0.146	0.695			
	+ Chl-a	10	-1531.2	861.9	775.7	0.152	0.672			
	*+ Age * Bonney UI*	*11*	*-2392.2*	*0.8*	*1207.2*	*0.147*	*0.696*	*0.0001*	*0.0001*	*1.080*
	+ Age * Bottom Temp	11	-2377.7	15.3	1199.9	0.147	0.696			
	+ Age * Chl-a	11	-1541.1	851.9	781.7	0.154	0.673			
Li:Ca	+ Growth	10	1056.1	198.5	-518.0	0.184	0.706			
	+ Bonney UI	11	1047.3	189.6	-512.6	0.191	0.709			
	+ Bottom Temp	11	1055.5	197.9	-516.7	0.186	0.706			
	+ Chl-a	**11**	**857.7**	**0.0**	**-417.7**	**0.204**	**0.693**	**0.1416**	**0.0324**	**4.373**
	+ Age * Bonney UI	12	1043.0	185.4	-509.4	0.197	0.709			
	+ Age * Bottom Temp	12	1053.2	195.5	-514.5	0.188	0.706			
	*+ Age * Chl-a*	*12*	*859.4*	*1.7*	*-417.6*	*0.207*	*0.693*	*-0.0424*	*0.0795*	*-0.534*
Growth	+ Growth	9	-1821.4	63.2	919.7	0.699	0.924			
	+ Bonney UI	*10*	*-1849.2*	*35.3*	*934.7*	*0.710*	*0.924*	*0.0006*	*0.0001*	*6.350*
	+ Bottom Temp	10	-1839.4	45.2	929.7	0.703	0.925			
	+ Chl-a	10	-1018.5	866.1	519.3	0.698	0.928			
	+ Age * Bonney UI	**11**	**-1884.6**	**0.0**	**953.3**	**0.713**	**0.925**	**0.0011**	**0.0002**	**6.480**
	+ Age * Bottom Temp	11	-1837.5	47.1	929.8	0.703	0.925			
	+ Age * Chl-a	11	-1020.2	864.3	521.2	0.698	0.928			

1050

Notes: Environmental variables were fitted to each optimal model with maximum likelihood (ML). Best explanatory variable or combination of variables is highlighted in **bold,** and were assessed using Akaike's information criterion corrected for small sample sizes (AICc). The second ranked variable(s) is *italicized*. Marginal (m) and conditional (c) R^2 values were calculated after models were refit with restricted maximum likelihood (REML). Parameter estimates and test statistics are displayed for the top and second ranked models. Interactions are designated with an asterisk (*).

Figure Legends:

Figure 1. Hypothesized correlations between age-corrected element:Ca ratios and estimated growth within otoliths and among individuals. Some otolith traits are correlated via physiological or environmental pathways. Solid arrows: within individual correlations; Dashed arrows: among individual correlations.

Figure 2. a) Map of the southeastern coast of South Australia during an upwelling event in January 2014. The strongest area of upwelling occurs off the Bonney Coast region where ocean perch otoliths were collected (dashed white line). Sea surface temperatures range from 14°C (dark blue) to 25°C (red). b) Ventral lobe of a thin-sectioned ocean perch otolith with dual laser transects (highlighted in blue) from low element concentration (LC) and high element concentration (HC) scans. Transects run from the otolith's core to the proximal edge. This fish was 5+ years old when collected in 2011 (tics on blue lines mark each annual growth increment). [SST image credit: Data were sourced from the Integrated Marine Observing System (IMOS) - IMOS is a national collaborative research infrastructure, supported by Australian Government]

Figure 3. Predicted monthly variation in otolith trace elements (element:Ca; µmol/mol) and average growth (Growth; µm) of ocean perch from the Bonney upwelling region. Power functions shown describe element:Ca assimilation rate (AR; $\mu mol \cdot mol^{-1} \cdot month^{-1}$) or growth rate (GR; µm/month). Note: scale of y-axis varies among panels. Data back-transformed to the original scale to aid interpretation.

Figure 4. Monthly resolved otolith trace elements (ratioed to calcium) and average growth predicted for ocean perch in the Bonney upwelling region off South Australia. Chronologies (solid lines) are produced from the *Month* random effect term (best linear unbiased predictors 'BLUPs'), with positive (negative) values indicating months of above (below) average assimilation/growth. The regional upwelling index (dotted line) is plotted on the secondary Y axis for reference.

Figure 5. Predicted effects for each element:Ca and average growth resulting from the best additive environmental effect model (a-c, g-h: left panels; dotted lines: ± SE) and the best environmental interaction with *Age* model (d-f, k-l: right panels). An asterisk in the upper

right corner indicates the top ranked model as selected by AICc values (ΔAICc = 0; shown in Table 4). Data back-transformed to original scale to aid interpretation.

Figure 6: a) Supported correlations within (solid lines) and among (dashed lines) individuals (point estimate credible intervals not spanning zero) from Figure 1 based on the multivariate model. Full correlation matrices are found in Tables S1 and S2. b) Within individual correlations as in (**a**) but with intrinsic variables removed from the multivariate model (full correlation matrix: Table S3). c) Among individual correlations when intrinsic variables removed from the multivariate model (full correlation matrix: Table S4). Correlation direction denoted by + or - and correlation strength by line color. Note correlation strength is much greater in (**c**) than in (**a**) or (**b**).

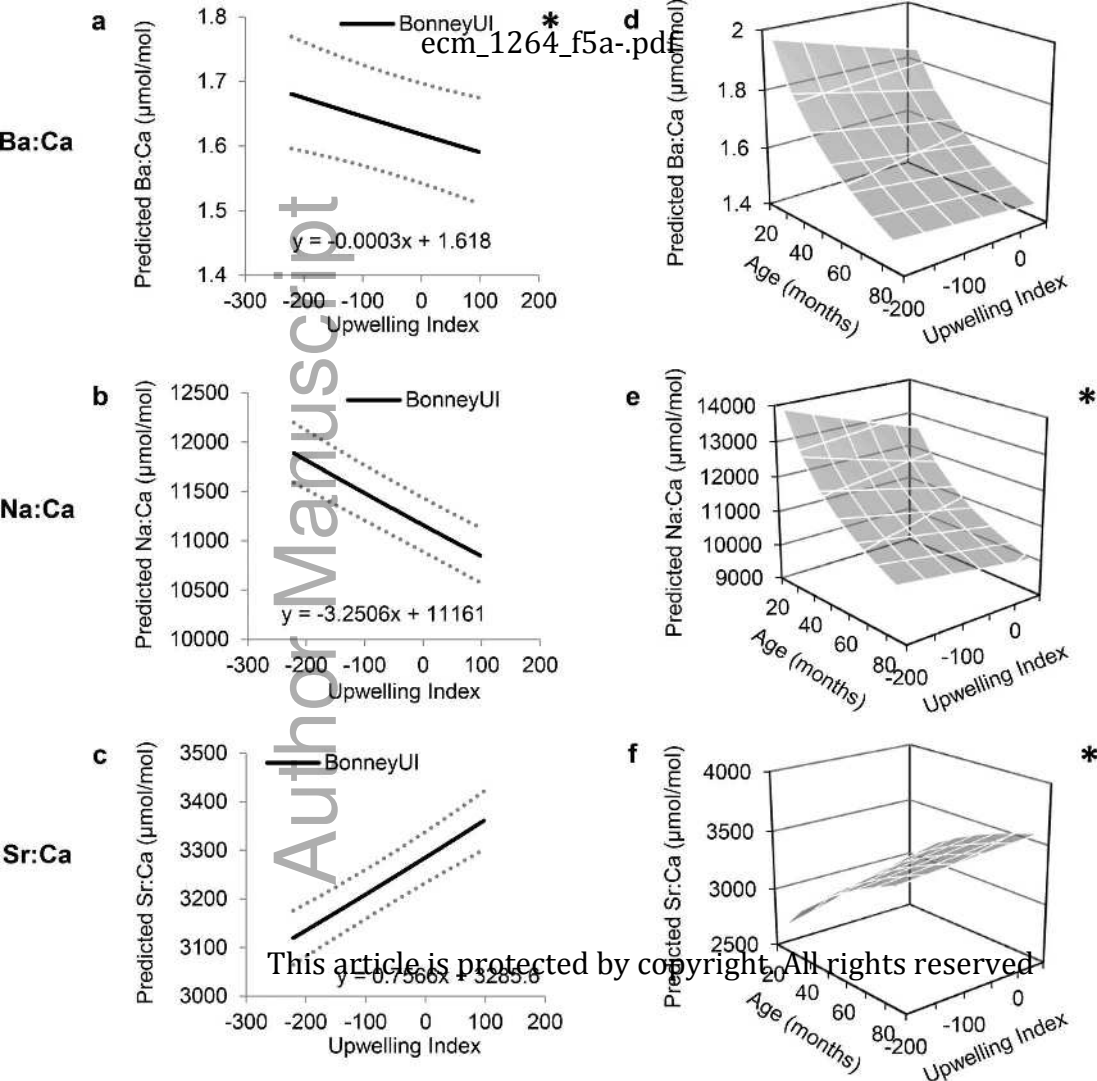

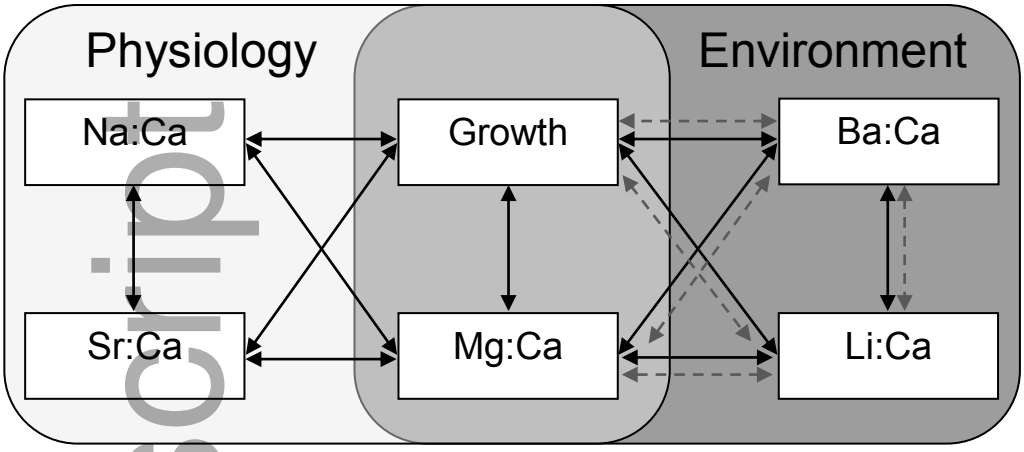

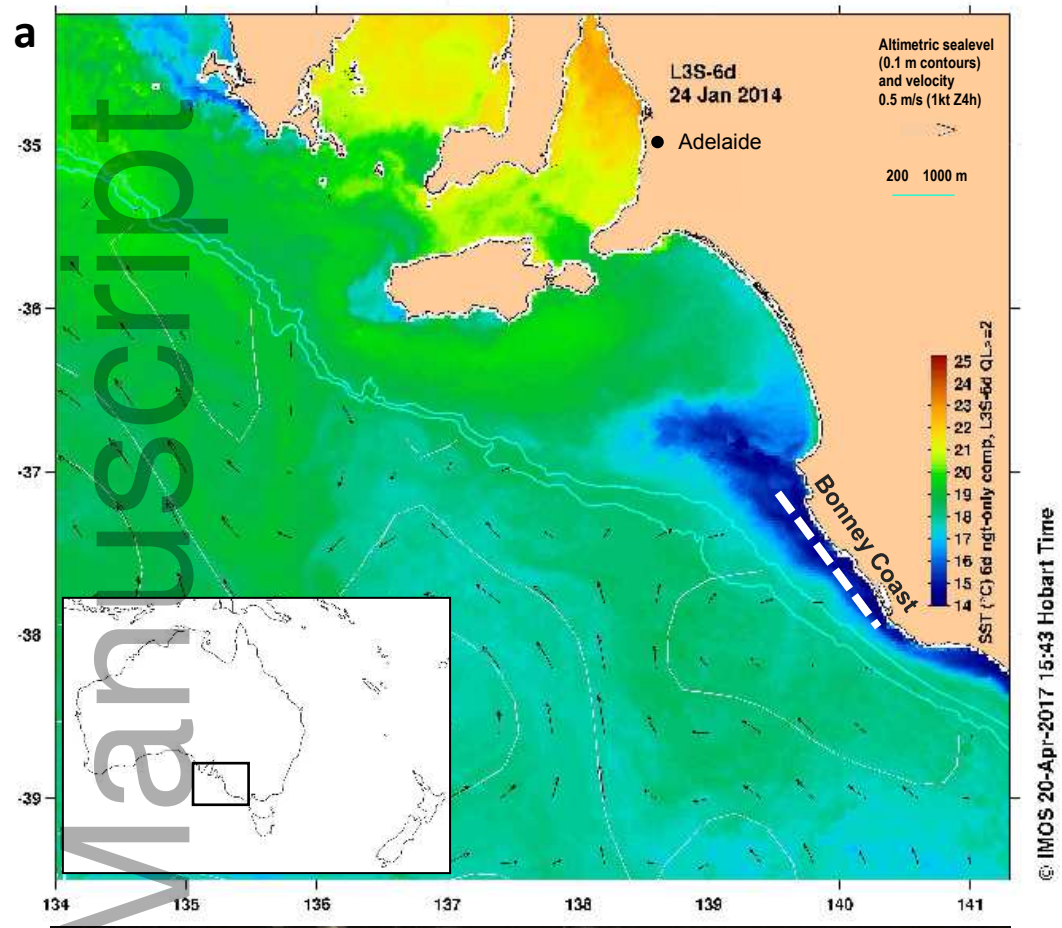

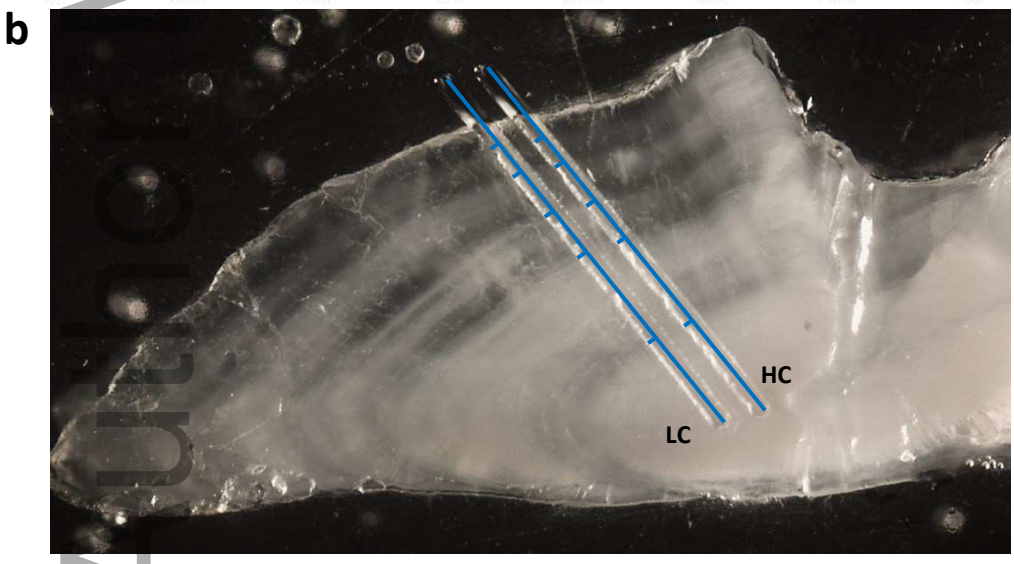

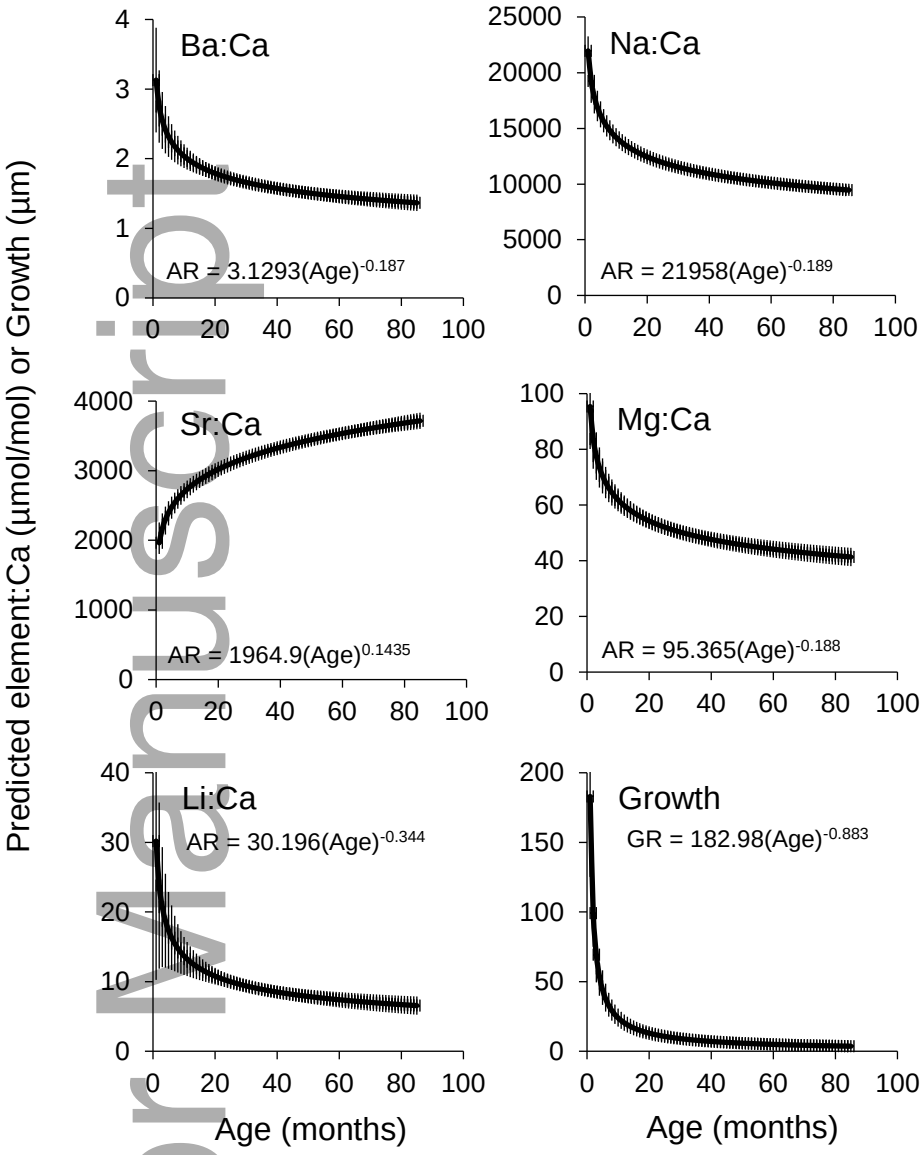

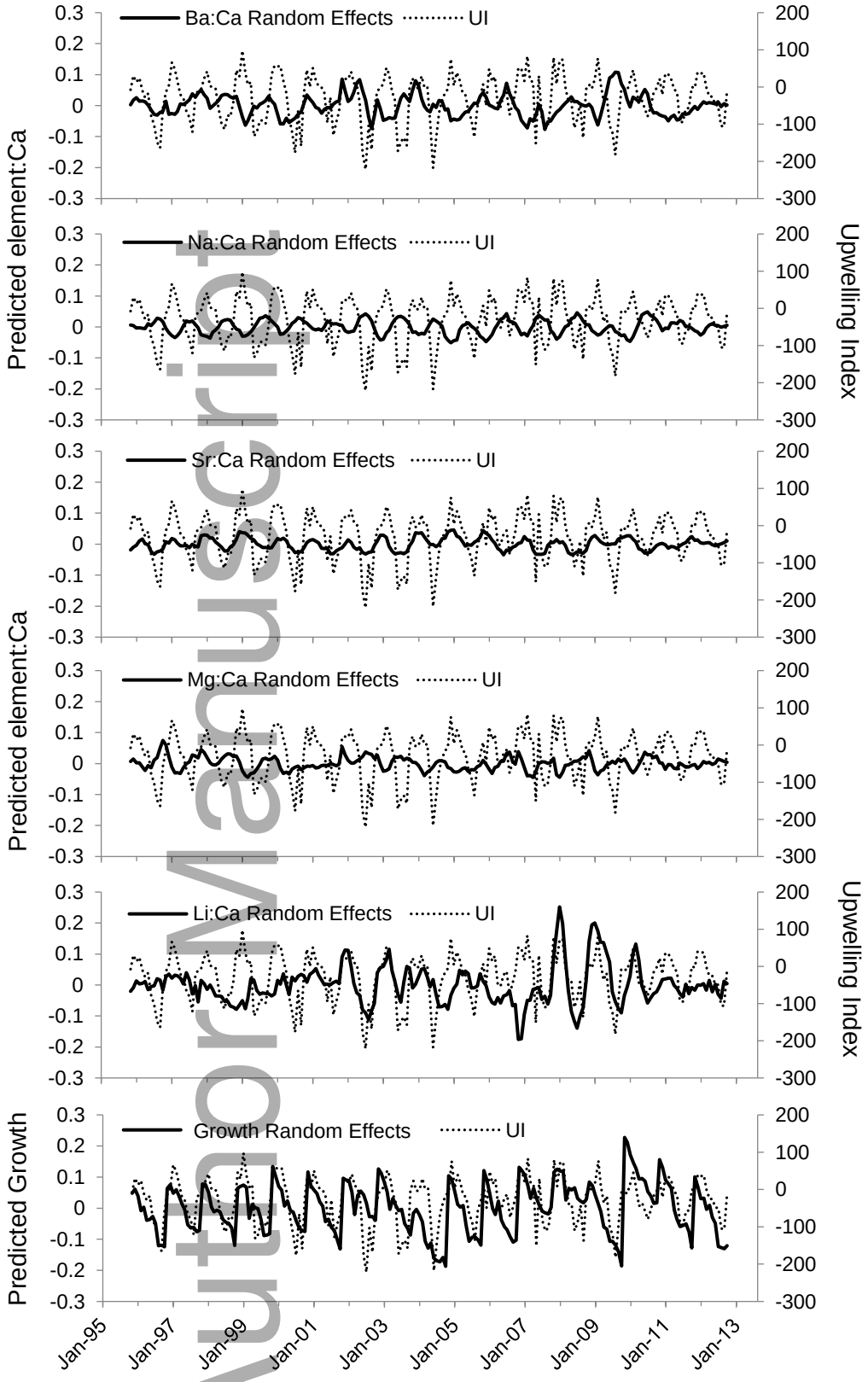

Mg:Ca

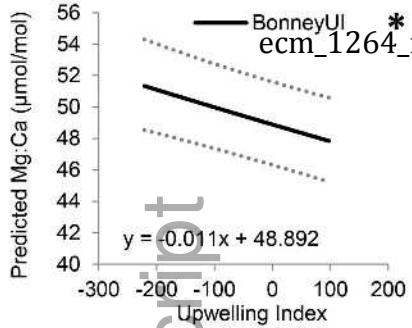

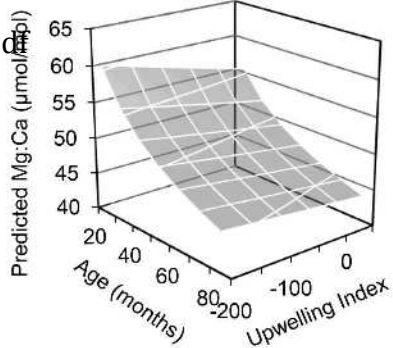

Li:Ca

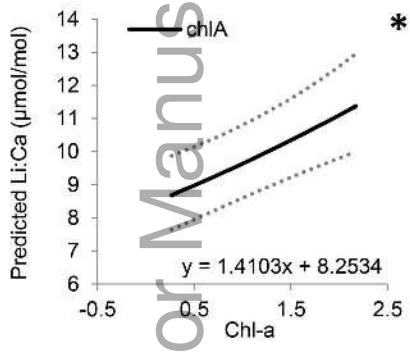

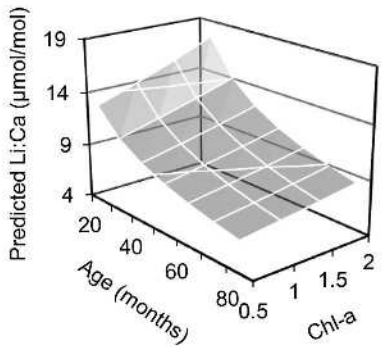

Growth

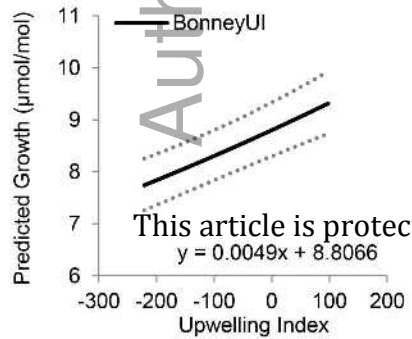

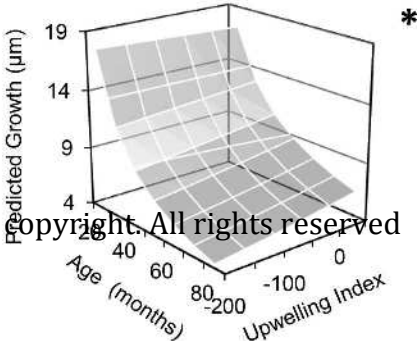

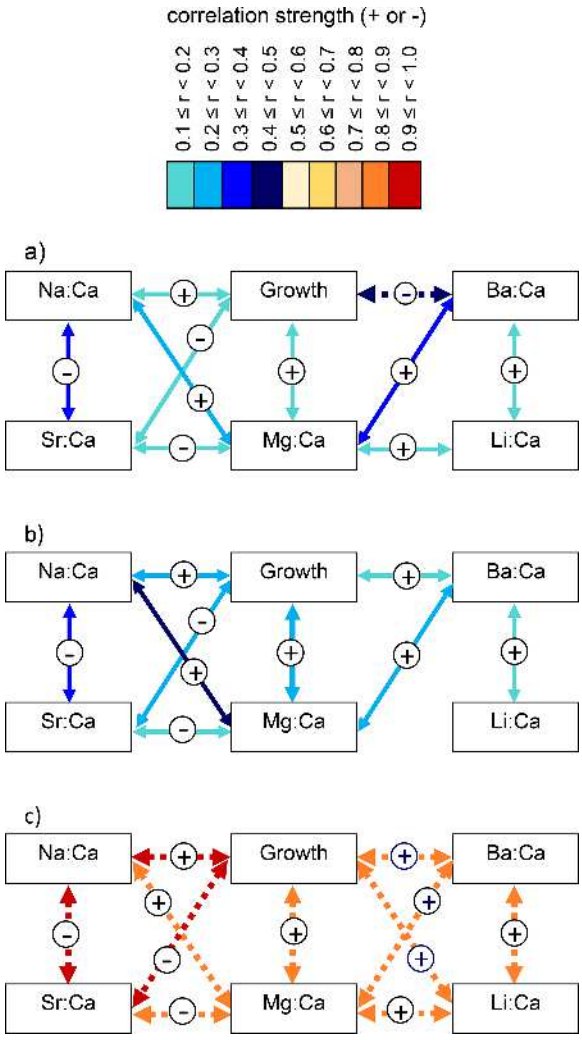

ecm_1264_f6.tif